THERMAL DIFFUSE X-RAY SCATTERING IN SIMPLE METALS*

BY

David M. Straus and N. W. Ashcroft

Laboratory of Atomic and Solid State Physics

and

Materials Science Center

Cornell University, Ithaca, New York 14853

Report #2559

Issued by the Materials Science Center

November 1975

Thermal Diffuse x-Ray Scattering in Simple Metals*

by

David M. Straus and N. W. Ashcroft

Laboratory of Atomic and Solid State Physics

and Materials Science Center

Cornell University, Ithaca, N.Y. 14853

Abstract

Calculations are reported for the ionic structure factor and x-ray scattering cross section of sodium (at T=0°K and 90°K) and lithium (both isotopes at T=0°K) within the harmonic approximation. An evaluation of the appropriate displacement- displacement correlation function by the special point method circumvents the need for a multiphonon expansion. In the case of sodium, the structure in the one-phonon scattering is straightforwardly accounted for, and an approximate expansion is obtained for all multiphonon scattering. By treating core and conduction electrons on an equal footing it is shown that information on the conduction electron system is present in the forward scattering component. In lithium the one-phonon cross section at small angles aids in the determination of the effective electron-ion interaction.

I INTRODUCTION

For some years x-ray thermal diffuse scattering (TDS) has been used as a probe of lattice dynamics in simple materials.[1-4] Although information on the phonon frequencies and polarizations (and also the extent of anharmonicity) is contained in the TDS,[4,5] it is generally hard to extract.[6] The cross section for the scattering of x rays intimately involves the static structure factor of the ions, $S_{ion}(\underset{\sim}{k})$.[7] The purpose of this paper is to present calculations of (i) $S_{ion}(\underset{\sim}{k})$; and (ii) the x-ray scattering cross section for Na and Li in the harmonic approximation and in their ground states. The significant features of the calculation are the use of a special point technique[8,9] in the computation of the equal time displacement-displacement correlation function $\langle \underset{\sim}{u}_i \underset{\sim}{u}_j \rangle$ (which enters into $S_{ion}(\underset{\sim}{k})$) and the separation of the scattering cross section into contributions from core and valence electrons. In particular, the special point technique enables us to avoid the customary expansion[4] of the inelastic part of $S_{ion}(\underset{\sim}{k})$ into terms involving the scattering of a definite number of phonons. We determine the "one-phonon" term explicitly, but we can also calculate <u>all</u> higher order processes without recourse to expansion. Further, our treatment of the contribution of the valence electrons to the cross section shows that x-ray scattering should yield information, in light metals, on the effective electron-ion interaction, as we demonstrate for the particular case of Li.

Section II contains a derivation of the x-ray scattering cross section $d\sigma/d\Omega$ in a model of a simple metal which distinguishes between bound and conduction electrons. In Sec. III we outline the calculation of $S_{ion}(\underset{\sim}{k})$ using the special point technique (discussed in detail in the Appendix), and compare it with the other non-expansion techniques in the literature. Section IV presents numerical results for $S_{ion}(\underset{\sim}{k})$ and $d\sigma/d\Omega$ for Na (at two temperatures)

and for both isotopes of Li. We draw particular attention to the secondary maxima associated with the one-phonon term as observed in certain crystallographic directions. These maxima have special importance in the determination of the electron-ion interaction of Li, and also give information about specific portions of the phonon spectrum directly.

II. THEORY

The differential cross section for scattering of a photon from a solid of N ions in volume V (at T = 0°K) is proportional to the space-time Fourier transform of the Van Hove correlation function $G_e(\underset{\sim}{r},t)$:

$$\frac{d^2\sigma}{d\Omega d\omega} = \frac{C}{V}\int d^3r \int_{-\infty}^{\infty} dt\ G_e(\underset{\sim}{r},t)\exp[i\underset{\sim}{k}\cdot\underset{\sim}{r} - i\omega t], \tag{2.1}$$

where C is a constant,[10-12]

$$G_e(\underset{\sim}{r},t) = \int d^3x \left\langle \hat{n}(\underset{\sim}{x},0)\hat{n}(\underset{\sim}{x}+\underset{\sim}{r},t)\right\rangle, \tag{2.2}$$

and

$$\underset{\sim}{k} = \underset{\sim}{k}_i - \underset{\sim}{k}_f; \qquad \omega = \omega_i - \omega_f. \tag{2.3}$$

We are considering the cross section per unit volume for scattering a photon of momentum $\hbar k_i$ and energy $\hbar\omega_i$ into a solid angle $d\Omega$ with energy loss between $\hbar\omega$ and $\hbar(\omega + d\omega)$. The quantities $\hbar k_f$ and $\hbar\omega_f$ are respectively the momentum and energy of the scattered photon. In Eq. (2.2) $\hat{n}(\underset{\sim}{r},t)$ is the total electron number density operator and the brackets $\langle\ \rangle$ refer to a ground state average. Introducing spatial Fourier transforms,

$$\frac{d^2\sigma}{d\Omega d\omega} = \frac{C}{V}\int_{-\infty}^{\infty} dt\ e^{-i\omega t} \left\langle \hat{n}(-\underset{\sim}{k},0)\hat{n}(\underset{\sim}{k},t)\right\rangle, \tag{2.4}$$

where $\hat{n}(\underset{\sim}{k})$ is the Fourier transform of $\hat{n}(r)$.

We separate $\hat{n}(\underset{\sim}{r})$ into contributions from core and valence electrons, and we treat the core electrons as if they were rigidly attached to the ions. Any core excitations or distortions of the ions are therefore neglected; should these occur they must be calculated separately. In practical terms this means that in comparing experiment and theory the Compton scattering from the <u>core</u> electrons must first be

subtracted from the data. In addition we invoke the adiabatic approximation, so that the conduction electrons (ce) are always in a ground state appropriate to an instantaneous ion configuration (ion). By virtue of the rigid ion approximation we may write:

$$\hat{n}(\underset{\sim}{k},t) = \sum_i e^{i\underset{\sim}{k}\cdot\underset{\sim}{R}_i(t)} f(\underset{\sim}{k}) + \hat{n}_{ce}(\underset{\sim}{k},t). \tag{2.5}$$

Here f(k) is the Fourier transform of the average core electron density about a nucleus at the origin, and $\underset{\sim}{R}_i(t)$ refers to the instantaneous position of the ion labelled i. From Eqs. (2.4), (2.5) and the adiabatic approximation, we then find:

$$\frac{d^2\sigma}{d\Omega d\omega}\cdot\frac{V}{C} = \int_{-\infty}^{\infty} dt e^{-i\omega t}\Big(\Big\langle \sum_{ij} e^{-i\underset{\sim}{k}\cdot\underset{\sim}{R}_i(0)}\, e^{i\underset{\sim}{k}\cdot\underset{\sim}{R}_j(t)} \Big\rangle_{ion} |f(\underset{\sim}{k})|^2$$

$$+ \Big\langle \sum_i e^{-i\underset{\sim}{k}\cdot\underset{\sim}{R}_i(0)}\, f(-\underset{\sim}{k}) \Big\langle \hat{n}_{ce}(\underset{\sim}{k},t)\Big\rangle_{ce}\Big\rangle_{ion}$$

$$+ \Big\langle \sum_i e^{i\underset{\sim}{k}\cdot\underset{\sim}{R}_i(t)}\, f(\underset{\sim}{k}) \Big\langle \hat{n}_{ce}(-\underset{\sim}{k},0)\Big\rangle_{ce}\Big\rangle_{ion}\Big)$$

$$+ \int_{-\infty}^{\infty} dt\, e^{-i\omega t} \Big\langle \hat{n}_{ce}(-\underset{\sim}{k},0)\, \hat{n}_{ce}(\underset{\sim}{k},t)\Big\rangle_{ce,ion}. \tag{2.6}$$

We suppose that the interaction between conduction electrons and ions can be represented by a weak pseudopotential with Fourier transform $\hat{v}(\underset{\sim}{k})$, (as is the case for many simple metals). The density response may then be calculated to linear order in $v(\underset{\sim}{k})$:

$$\Big\langle \hat{n}_{ce}(\underset{\sim}{k},t)\Big\rangle_{ce} = \chi_1(\underset{\sim}{k})\, v(\underset{\sim}{k}) \sum_i e^{i\underset{\sim}{k}\cdot\underset{\sim}{R}_i(t)}, \tag{2.7}$$

with

$$\chi_1(\underset{\sim}{k}) = \frac{k^2}{4\pi e^2}\left(\frac{1}{\epsilon(\underset{\sim}{k},0)} - 1\right). \tag{2.8}$$

$\epsilon(\underset{\sim}{k},0)$ being the static dielectric function of the uniform interacting electron gas.[13] Equations (2.6), (2.7) and (2.8) now give:

$$\frac{d^2\sigma}{d\Omega d\omega} \cdot \frac{V}{C} = \int_{-\infty}^{\infty} dt e^{-i\omega t} \left[\left\langle \sum_{ij} e^{-i\underset{\sim}{k}\cdot(\underset{\sim}{R}_i(0)-\underset{\sim}{R}_j(t))} \right\rangle_{ion} (|f(\underset{\sim}{k})|^2 + 2f(\underset{\sim}{k})\chi_1(\underset{\sim}{k})v(\underset{\sim}{k})) \right.$$

$$\left. + \left\langle \hat{n}_{ce}(-\underset{\sim}{k},0)\hat{n}_{ce}(\underset{\sim}{k},t) \right\rangle_{ce,ion} \right]. \qquad (2.9)$$

In a typical x-ray experiment <u>all</u> the radiation emerging at a given angle is initially measured.[14] All possible energy transfers (on the scale of typical electron and phonon energies) $\hbar\omega$ are therefore included, and we pass from the cross-section for energy loss $\hbar\omega$ $(d^2\sigma/d\Omega d\omega)$ to the total angular cross section $(d\sigma/d\Omega)$:

$$\frac{d\sigma}{d\Omega} = \int_{-\infty}^{\infty} d\omega \frac{d^2\sigma}{d\Omega d\omega} = 2\pi\frac{C}{V} \left[\left\langle \sum_{ij} e^{-i\underset{\sim}{k}\cdot(\underset{\sim}{R}_i-\underset{\sim}{R}_j)} \right\rangle_{ion} (|f(\underset{\sim}{k})|^2 + 2f(\underset{\sim}{k})\chi_1(\underset{\sim}{k})v(\underset{\sim}{k})) \right.$$

$$\left. + \left\langle \hat{n}_{ce}(-\underset{\sim}{k})\, \hat{n}_{ce}(\underset{\sim}{k}) \right\rangle_{ce,ion} \right]. \qquad (2.10)$$

Note that the last term is usually considered part of the Compton scattering, and is therefore generally subtracted from the primary data.[16] What will become apparent in Sec. IV, is that the value of the last term in Eq. (2.10) (the valence electron correlation function) should be readily obtainable from x-ray measurements. The theoretical results we present are therefore best compared to data from which only the <u>ionic</u> Compton scattering has been subtracted.

The last term in Eq. (2.10) is difficult to calculate for interacting electrons in the presence of the ions. For purposes of illustration we use the free-electron value[13,17]:

$$N_e S_e(\underset{\sim}{k}) \equiv \left\langle \hat{n}_{ce}(-\underset{\sim}{k})\hat{n}_{ce}(\underset{\sim}{k}) \right\rangle_{ce,free} ,$$

$$S_e(\underset{\sim}{k}) = \left(\frac{3k}{4k_f} - \frac{1}{16}\frac{k^3}{k_f^3} \right), \qquad 0 < k \leq 2k_f; \qquad (2.11)$$

$$= 1, \qquad k \geq 2k_f.$$

Here N_e is the number of electrons, and k_f the Fermi wave vector. Setting (for a monovalent system) the number of electrons N_e equal to the number of ions N, Eq.s (2.10) and (2.11) give us the final result:

$$W \equiv \frac{d\sigma}{d\Omega} \cdot \frac{V}{N} \cdot \frac{1}{2\pi C} = S_{ion}(\underset{\sim}{k}) \cdot (|f(\underset{\sim}{k})|^2 + 2f(\underset{\sim}{k})\chi_1(\underset{\sim}{k})v(\underset{\sim}{k})) + S_e(\underset{\sim}{k}), \quad (2.12)$$

where we have set

$$S_{ion}(\underset{\sim}{k}) = \frac{1}{N}\left\langle \sum_{ij} e^{-i\underset{\sim}{k}\cdot(\underset{\sim}{R}_i - \underset{\sim}{R}_j)} \right\rangle_{ion} \quad \text{for } \underset{\sim}{k} \neq 0. \quad (2.13)$$

It should be clear that except for the elements of lowest atomic number (e.g. Li), $S_e(\underset{\sim}{k})$ makes a small contribution to W for all but the smallest wave vectors $k < 2k_f$.

III CALCULATION OF IONIC STRUCTURE FACTOR

We now proceed to a calculation of $S_{ion}(\underset{\sim}{k})$ in a model in which the solid is treated as a harmonic crystal. Letting $\underset{\sim}{R}_i = \underset{\sim}{X}_i + \underset{\sim}{u}_i$, where $\underset{\sim}{X}_i$ is the equilibrium position of the i^{th} ion and $\underset{\sim}{u}_i$ its displacement,

$$S_{ion}(\underset{\sim}{k}) = \frac{1}{N} \sum_{ij} e^{-i\underset{\sim}{k}\cdot\underset{\sim}{X}_{ij}} \left\langle e^{-i\underset{\sim}{k}\cdot(\underset{\sim}{u}_i - \underset{\sim}{u}_j)} \right\rangle_{ion} . \tag{3.1}$$

Here, $\underset{\sim}{X}_{ij} = \underset{\sim}{X}_i - \underset{\sim}{X}_j$, and the average is to be taken over the states appropriate to a harmonic crystal. With the definitions

$$\left\langle (u_i - u_j)_\alpha \, (u_i - u_j)_\beta \right\rangle_{ion} \equiv \lambda_{\alpha\beta} \, (\underset{\sim}{X}_i - \underset{\sim}{X}_j) \tag{3.2}$$

and

$$\underset{\sim}{u} = (u_1, u_2, u_3),$$

we have the result[4,19]:

$$\left\langle e^{-i\underset{\sim}{k}\cdot(\underset{\sim}{u}_i - \underset{\sim}{u}_j)} \right\rangle_{ion} = e^{-\frac{1}{2}k_\alpha k_\beta \lambda_{\alpha\beta}(\underset{\sim}{X}_i - \underset{\sim}{X}_j)} , \tag{3.3}$$

where

$$\lambda_{\alpha\beta}(\underset{\sim}{X}_i - \underset{\sim}{X}_j) = \frac{\hbar}{MN} \sum_{\underset{\sim}{q}j}^{BZ} (1-\cos \underset{\sim}{q}\cdot\underset{\sim}{X}_{ij}) e_\alpha(\underset{\sim}{q}j) e_\beta(\underset{\sim}{q}j) \frac{1}{\omega(\underset{\sim}{q}j)} \coth[\tfrac{1}{2}\beta\hbar\omega(\underset{\sim}{q}j)],$$

$$\beta = 1/k_B T, \tag{3.4}$$

and M is the mass of an ion. In Eq.(3.4) $\omega(\underset{\sim}{q}j)$ and $\underset{\sim}{e}(\underset{\sim}{q}j)$ are the frequency and polarization vector of the normal mode of wave vector $\underset{\sim}{q}$ and polarization index j, (j=1,2,3). The $\underset{\sim}{q}$ sum extends over the entire first Brillouin zone. Using the translational symmetry of the lattice, Eqs. (3.1)-(3.4) yield:

$$S_{ion}(\underset{\sim}{k}) = \sum_i e^{-i\underset{\sim}{k}\cdot\underset{\sim}{X}_i} \; e^{-\frac{1}{2}k_\alpha k_\beta \lambda_{\alpha\beta}(\underset{\sim}{X}_i)} . \tag{3.5}$$

Next we separate $\lambda_{\alpha\beta}(\underset{\sim}{X}_i)$ as follows:

$$\lambda_{\alpha\beta}(\underset{\sim}{X}_i) = \Lambda_{\alpha\beta}(0) \quad - \quad \Lambda_{\alpha\beta}(\underset{\sim}{X}_i), \tag{3.6}$$

with

$$\Lambda_{\alpha\beta}(\underset{\sim}{X}_i) = \frac{\hbar}{MN} \sum_{\underset{\sim}{q}j} e_\alpha(\underset{\sim}{q}j) e_\beta(\underset{\sim}{q}j) \frac{1}{\omega(\underset{\sim}{q}j)} \coth\left[\tfrac{1}{2}\beta\hbar\omega(\underset{\sim}{q}j)\right] \cos\left(\underset{\sim}{q}\cdot\underset{\sim}{X}_i\right). \tag{3.7}$$

Note that

$$\Lambda_{\alpha\beta}(\underset{\sim}{X}_{ij}) = 2 \left\langle u_{i\alpha}\, u_{j\beta} \right\rangle_{\text{ion}}. \tag{3.8}$$

We see therefore that $\Lambda_{\alpha\beta}(\underset{\sim}{X})$ is the displacement-displacement correlation function for two ions separated (on average) by $\underset{\sim}{X}$. Clearly $\Lambda_{\alpha\beta}(0)$ is the displacement-displacement autocorrelation function. For a cubic system,

$$\left\langle u_{i\alpha}\, u_{i\beta} \right\rangle_{\text{ion}} = \delta_{\alpha\beta} \frac{1}{3} \left\langle \underset{\sim}{u}_i \cdot \underset{\sim}{u}_i \right\rangle, \tag{3.9}$$

so that

$$\Lambda_{\alpha\beta}(0) = \delta_{\alpha\beta} \frac{1}{3} \frac{\hbar}{MN} \sum_{\underset{\sim}{q}j} \frac{1}{\omega(\underset{\sim}{q}j)} \coth\left[\tfrac{1}{2}\beta\hbar\omega(\underset{\sim}{q}j)\right] \equiv \delta_{\alpha\beta}\, \Lambda^o. \tag{3.10}$$

This defines Λ^o, which is closely related to the Debye-Waller[4] factor e^{-2W}:

$$2W = \tfrac{1}{2} k_\alpha k_\beta \Lambda_{\alpha\beta}(0) = \tfrac{1}{2} k^2 \Lambda^o. \tag{3.11}$$

Substituting Eqs. (3.6)-(3.11) into Eq.(3.5), we find:

$$\begin{aligned} S_{\text{ion}}(\underset{\sim}{k}) &= \sum_i e^{-i\underset{\sim}{k}\cdot\underset{\sim}{X}_i}\, e^{-\frac{1}{2}k_\alpha k_\beta [\Lambda_{\alpha\beta}(0) \,-\, \Lambda_{\alpha\beta}(\underset{\sim}{X}_i)]} \\ &= \sum_i e^{-i\underset{\sim}{k}\cdot\underset{\sim}{X}_i}\, e^{-\frac{1}{2}k^2\Lambda^o}\, e^{+\frac{1}{2}k_\alpha k_\beta \Lambda_{\alpha\beta}(\underset{\sim}{X}_i)}. \end{aligned} \tag{3.12}$$

To proceed from this point the usual approach is to expand the last exponential in a power series in $\Lambda_{\alpha\beta}(\underset{\sim}{X}_i)$. The leading (i.e. constant) term

gives the elastic (Bragg) scattering peaks, the second gives the one-phonon scattering, the third the two-phonon scattering, and so forth. Beyond the one-phonon contribution each term is increasingly laborious to evaluate. We can avoid this expansion, however, by writing $S_{ion}(\underset{\sim}{k})$ as follows:

$$S_{ion}(\underset{\sim}{k}) = \sum_i e^{-i\underset{\sim}{k}\cdot\underset{\sim}{X}_i} e^{-\frac{1}{2}k^2\Lambda^o} + \sum_i e^{-i\underset{\sim}{k}\cdot\underset{\sim}{X}_i} e^{-\frac{1}{2}k^2\Lambda^o} [\tfrac{1}{2}k_\alpha k_\beta \Lambda_{\alpha\beta}(\underset{\sim}{X}_i)]$$

$$+ \sum_i e^{-i\underset{\sim}{k}\cdot\underset{\sim}{X}_i} e^{-\frac{1}{2}k^2\Lambda^o} [e^{\frac{1}{2}k_\alpha k_\beta \Lambda_{\alpha\beta}(\underset{\sim}{X}_i)} - 1 - \tfrac{1}{2}k_\alpha k_\beta \Lambda_{\alpha\beta}(\underset{\sim}{X}_i)]$$

$$\equiv S_o(\underset{\sim}{k}) + S_1(\underset{\sim}{k}) + S_M(\underset{\sim}{k}). \tag{3.13}$$

Here $S_o(\underset{\sim}{k})$ gives the elastic scattering,

$$\text{i.e.} \quad S_o(\underset{\sim}{k}) = Ne^{-\frac{1}{2}k^2\Lambda^o} \sum_{\underset{\sim}{K}} \delta_{\underset{\sim}{k},\underset{\sim}{K}}, \tag{3.14}$$

the $\underset{\sim}{K}$ being the vectors of the reciprocal lattice. The one-phonon scattering term $S_1(\underset{\sim}{k})$ is easily seen to be:

$$S_1(\underset{\sim}{k}) = e^{-\frac{1}{2}k^2\Lambda^o} \frac{\hbar}{2M} k_\alpha k_\beta \sum_j e_\alpha[\underset{\sim}{q}(\underset{\sim}{k})j]\, e_\beta[\underset{\sim}{q}(\underset{\sim}{k})j] \frac{1}{\omega[\underset{\sim}{q}(\underset{\sim}{k})j]} \coth\left[\tfrac{1}{2}\hbar\beta\omega[\underset{\sim}{q}(\underset{\sim}{k})j]\right], \tag{3.15}$$

where $\underset{\sim}{q}(\underset{\sim}{k})$ is the vector $\underset{\sim}{k}$ reduced by an appropriate $\underset{\sim}{K}$ to the first Brillouin zone (i.e., $\underset{\sim}{q}(\underset{\sim}{k}) = \underset{\sim}{k} - \underset{\sim}{K}$). Finally the remainder $S_M(\underset{\sim}{k})$ will be calculated by direct computation of $\Lambda_{\alpha\beta}(\underset{\sim}{X}_i)$, so that all higher order phonon terms are automatically taken into account. The reason for adopting this procedure is to assure convergence in the sum over i in $S_M(\underset{\sim}{k})$. This will be clarified in what follows.

Our method of calculation of $\Lambda_{\alpha\beta}(\underset{\sim}{R}_i)$ and Λ^o makes use of special points in the first Brillouin zone[8,9] to evaluate the integral of Eq.(3.7). By calculating the integrand at these relatively few special points, one obtains a good approximation to the entire integral. This procedure differs markedly

from ordinary numerical integration in that (as shown in the Appendix) one is effectively using an expansion of the integrand in symmetrized plane waves. In connection with this method we draw attention to the behavior of $\Lambda_{\alpha\beta}(\underset{\sim}{X})$ for large $\underset{\sim}{X}$. At large $\underset{\sim}{X}$ the dominant contribution to the integral in Eq.(3.7) comes from small $\underset{\sim}{q}$, and it can be shown[20] that at T=0°K,

$$\lim_{X\to\infty} \Lambda_{\alpha\beta}(\underset{\sim}{X}) \sim \frac{1}{X^2} \quad . \tag{3.16}$$

Thus to ensure convergence in $S_M(\underset{\sim}{k})$ it is necessary to make the separation indicated in Eq.(3.13).

The method may be compared with the non-expansion calculations of $S_{ion}(\underset{\sim}{k})$ by (1) Lomer,[21] who calculates the ionic structure factor directly using the results of a computer experiment; (2) Semenovskaya and Umanskii,[22] who calculate $\Lambda_{\alpha\beta}(\underset{\sim}{X})$ in closed form for a model sinusoidal phonon dispersion law; and (3) Reid and Smith,[23] who calculate the multi-phonon scattering $S_M(\underset{\sim}{k})$ for crystals whose sizes range between 100 and 1000 unit cells. Their evaluation of $\Lambda_{\alpha\beta}(\underset{\sim}{X})$ is acheived by summing over only those $\underset{\sim}{q}$ corresponding to the normal modes of such a finite crystal. By separately calculating the $\underset{\sim}{q}\to 0$ portion of the integral in Eq.(3.7), they find that a crystal of 500 unit cells gives essentially the same $S_M(\underset{\sim}{k})$ as an infinite crystal, for $\underset{\sim}{q}(\underset{\sim}{k})$ belonging to the set of normal modes of the finite crystal.

The method of Reid and Smith appears to be the most accurate and practical, but has the disadvantages that one can calculate $S_M(\underset{\sim}{k})$ at relatively few points, and that the matrices $\Lambda_{\alpha\beta}(\underset{\sim}{X})$ for a real crystal are inaccessible. We are able to circumvent these limitations by directly calculating the correlation matrices $\Lambda_{\alpha\beta}(\underset{\sim}{X})$. (These are of considerable interest, of course, in a wide range of problems.)

We illustrate the method by its application to Na and Li. In both cases the phonon spectrum was calculated from a force-constant model designed to fit the

experimental data. The corresponding $S_{ion}(\underset{\sim}{k})$ has been calculated for Na at two temperatures (0°K, 90°K) and for both isotopes of Li (at T=0°K).

In the case of Na the force constants were those that fit the data at T=90°K[24]. A simple estimate (supported by some theoretical results[25]) indicates that the change in phonon frequencies between 0°K and 90°K is everywhere less than the experimental error. Hence the only effect of temperature we allow is through the hyperbolic cotangent function in Eq.(3.7).[26] To simplify the calculation we use the T=0°K value of $\Lambda_{\alpha\beta}(\underset{\sim}{X}_i)$ for $\underset{\sim}{X}_i \neq 0$ in the 90°K calculation, but use the T=90°K value of $\Lambda_{\alpha\beta}(0)$.[27] The 90°K results are therefore meant to be indicative of the effects of temperature, but they are only approximate. We use the value of r_s determined from the 5°K lattice constant measurement,[28] i.e. $r_s = 3.931$ a.u. (r_s is defined by $\frac{4}{3}\pi(r_s a_o)^3 = \frac{V}{N_e}$, where a_o is the Bohr radius.)

The force constants for ^{7}Li were similarly taken to be those which fit the experimental phonon dispersion[29] measured at T = 98°K. The values of r_s was also deduced from the lattice constant,[28] in this case at 78°K ($r_s = 3.248$ a.u.). To calculate $S_{ion}(\underset{\sim}{k})$ we have set T=0°K. In order to obtain $S_1(\underset{\sim}{k})$, Λ^o, and $\Lambda_{\alpha\beta}(\underset{\sim}{X}_i)$ for ^{6}Li, we have assumed that both substances are truly harmonic. This gives:

$$\begin{aligned} \omega &\propto M^{-\frac{1}{2}}, \\ \Lambda_{\alpha\beta}(\underset{\sim}{X}) &\propto M^{-\frac{1}{2}} \text{ for all } \underset{\sim}{X}, \\ \text{and } S_1(\underset{\sim}{k}) &\propto M^{-\frac{1}{2}}. \end{aligned} \tag{3.17}$$

IV RESULTS

In this section we present numerical results for both $S_{ion}(\underset{\sim}{k})$ and the x-ray scattering cross sections for Na and Li. The structure factor calculations were carried out as described above. As regards the cross sections, we give two sets of results. One corresponds to the theory outlined in Sec. II:

$$W = \frac{d\sigma}{d\Omega} \cdot \frac{V}{N} \cdot \frac{1}{2\pi C} = S(\underset{\sim}{k})\left(|f(\underset{\sim}{k})|^2 + 2f(\underset{\sim}{k})\, \chi_1(\underset{\sim}{k})\, v(\underset{\sim}{k}) \right) + S_e(\underset{\sim}{k}) , \qquad (4.1)$$

while the other corresponds to the more commonly used expression:

$$W_a = \left(\frac{d\sigma}{d\Omega} \frac{V}{N} \frac{1}{2\pi C}\right)_a = S(\underset{\sim}{k})\, |f_a(\underset{\sim}{k})|^2 . \qquad (4.2)$$

Here $f_a(\underset{\sim}{k})$ is the Fourier transform of the average electron density of an assumed neutral atom, and we write (and shall continue to do so) $S(\underset{\sim}{k})$ in place of $S_{ion}(\underset{\sim}{k})$. Both the ionic ($Na^+$, Li^+) and the atomic (Na, Li) form factors were taken from Ref. 30. The Geldart and Vosko[31] modified form of the Hubbard dielectric function $\epsilon(\underset{\sim}{k})$ was used, as well as an empty core pseudopotential to represent the effective electron-ion interaction.[32] Figures 1-7 show $S(\underset{\sim}{k})$ for Na, and Figs. 8-10 show $S(\underset{\sim}{k})$ for both isotopes of Li. Numerical results are listed in Tables I-IV. We present both cross sections W and W_a for Na (at T = 0°K) in Figs. 12-15, and in Figs. 16-18 we show W for Li (at T = 0°K) with two choices of the core radius appearing in the empty core pseudopotential.

The most noticeable feature of the structure factor plots is the sizeable structure between the Bragg peaks along all directions except the [100] and [110] directions (for a bcc lattice). These maxima are a direct consequence of the behavior of the one-phonon term.[33] Their occurrence is completely general, and has been noted for quite some time.[34] For the sake of simplicity, however, we can most easily explain them in terms of a (polarization-independent)

Debye model. Here (at $T = 0°K$),

$$S_1(\underset{\sim}{k}) = e^{-\frac{1}{2}k^2\Lambda^o} \frac{\hbar}{2M} k^2 \frac{1}{\omega(\underset{\sim}{q}(\underset{\sim}{k}))} , \tag{4.3}$$

where $\omega(q) = cq$ is independent of polarization and c is the approximate speed of sound. We have plotted in Fig. 11 lines along which the function $1/c|\underset{\sim}{q}(\underset{\sim}{k})|$ has constant value for a (001) plane of the reciprocal lattice of a bcc crystal. In any direction (except [100] and [110]), and as a consequence of periodicity alone, the one-phonon term displays secondary maxima as one passes over the ridges of the function shown. Replacing Eq. (4.3) with Eq. (3.15) introduces three frequencies (one for each polarization j) at every point, each weighted by the factor $[\underset{\sim}{k}\cdot\underset{\sim}{e}(j\underset{\sim}{q}(\underset{\sim}{k}))]^2$. For example, Fig. 11 would indicate two secondary maxima between the points[37] (1,0,0) and (3,1,0), whereas Fig. 7 shows only one. The value of the one-phonon term at the point along [310] marked P on Figure 11 is determined by the phonons at the point $q = (\frac{1}{2},\frac{1}{2},0)$ in the first Brillouin zone. At $(\frac{1}{2},\frac{1}{2},0)$ Na has an anomalously low transverse frequency.[24] Furthermore, since q is nearly perpendicular to the [310] direction, the factor $\sum_j [\underset{\sim}{e}(jq)\cdot\underset{\sim}{k}]^2$ will select out the transverse frequencies. The resulting single, large, maximum swamps any other effects. Thus we see that any particularly low phonon frequency will cause a sequence of one-phonon maxima along the appropriate direction. This property of the one-phonon scattering has been widely used to study soft modes,[38] but the discussion is often set in real space. In terms of identifying the maximum with a particular vibrational mode we see that it is advantageous to treat the problem in reciprocal space.

The comparison of W and W_a for Na in Figs. 12-14 shows that at large $\underset{\sim}{k}$ the only significant difference is a shift arising from the term $S_e(\underset{\sim}{k})$ in W, which is a constant for $k > 2k_f$. However, at small $\underset{\sim}{k}$ Fig. 15 shows

that the presence of $S_e(\underset{\sim}{k})$ in W contributes to a difference in shape between W and W_a. The small $\underset{\sim}{k}$ portion of the x-ray cross section (with only ionic Compton scattering subtracted out) thus gives us information about the conduction electrons.[39] Note also that for Na the presence of the pseudopotential $v(\underset{\sim}{k})$ in W seems to make little difference in the final cross section. This is not so for elements of very low atomic number. For example, in Figs. 16 and 17 we plot W for ^{7}Li at low values of $\underset{\sim}{k}$, for two choices of the core radius appearing in the empty-core pseudopotential.[40] The maximum percentage difference is slight in both cases, but in Fig. 17 the actual shape of the one-phonon maximum is noticeably altered. In fact, the differences between pseudopotentials will always be most noticeable in low $\underset{\sim}{k}$ one-phonon maxima. In order for $v(\underset{\sim}{k})$ to have any influence in Eq. (4.1), we need to have $k < 2k_f$ (otherwise χ_1 is exceedingly small) and $S(\underset{\sim}{k})$ to be not too small. Figure 18 emphasizes this point: Here we plot $W - S_e(\underset{\sim}{k})$, so we subtract all the Compton scattering. What remains shows a marked dependence on the pseudopotential.

We should discuss the relative composition of the TDS (i.e. of $S(\underset{\sim}{k})$). Figure 1 shows the contribution of the one-phonon term, and we see that at large $\underset{\sim}{k}$ the many-phonon terms become quite important. From Eqs. (3.11) and (3.13)[41]:

$$S_M(\underset{\sim}{k}) = e^{-\frac{1}{2}k_\alpha k_\beta \Lambda_{\alpha\beta}(0)}\left[e^{\frac{1}{2}k_\alpha k_\beta \Lambda_{\alpha\beta}(0)} - 1 - \tfrac{1}{2}k_\alpha k_\beta \Lambda_{\alpha\beta}(0)\right]$$

$$+ \sum_{i\neq 0} e^{-i\underset{\sim}{k}\cdot\underset{\sim}{X}_i}\, e^{-\frac{1}{2}k_\alpha k_\beta \Lambda_{\alpha\beta}(0_i)}\left[e^{\frac{1}{2}k_\alpha k_\beta \Lambda_{\alpha\beta}(\underset{\sim}{X}_i)} - 1 - \tfrac{1}{2}k_\alpha k_\beta \Lambda_{\alpha\beta}(\underset{\sim}{X}_i)\right]. \qquad (4.4)$$

From the Appendix we also note that for Na, $\mathrm{Tr}\Lambda_{\alpha\beta}(\underset{\sim}{X}_i) << \mathrm{Tr}\Lambda_{\alpha\beta}(0)$ (for $\underset{\sim}{X}_i \neq 0$). Typically at least 90% of $S_M(\underset{\sim}{k})$ in Na comes from the first term in Eq. (4.4), i.e.;

$$S_M(\underset{\sim}{k}) \approx 1 - e^{-\frac{1}{2}k_\alpha k_\beta \Lambda_{\alpha\beta}(0)}\left[1 + \tfrac{1}{2}k_\alpha k_\beta \Lambda_{\alpha\beta}(0)\right]. \qquad (4.5)$$

In Eq. (4.5) we have confirmed a well known approximation.[36]

In spite of the fact that the $\underset{\sim}{X}_i$ sum in $S_M(\underset{\sim}{k})$ converges roughly as $\Sigma_i \, 1/X_i^4$, we have found it adequate to take only 9 shells (136 vectors) in the sum. (Taking only 7 shells changes $S(\underset{\sim}{k})$ for Na by considerably less than 1%, for example.) This can be understood by noting that

$$\mathrm{Tr}\Lambda_{\alpha\beta}(\underset{\sim}{X}_9) << \mathrm{Tr}\Lambda_{\alpha\beta}(\underset{\sim}{X}_1) << \mathrm{Tr}\Lambda_{\alpha\beta}(0), \tag{4.6}$$

where $\underset{\sim}{X}_1$ and $\underset{\sim}{X}_9$ are typical vectors in the first and ninth shells. The point is that the asymptotic limit of $\Lambda_{\alpha\beta}(\underset{\sim}{X}_i)$ ($\propto 1/X_i^2$) is only reached at large $\underset{\sim}{X}_i$ where the structure factor is almost independent of the contribution of the remaining shells. In addition, the $\underset{\sim}{X}_i$ sum actually converges more quickly than $\Sigma_i \, 1/X_i^4$ since the term $e^{-i\underset{\sim}{k}\cdot\underset{\sim}{X}_i}$ in Eq. (4.4) introduces (except for $\underset{\sim}{k} = \underset{\sim}{K}$) considerable self-cancellation.

V DISCUSSION

The extension of our method of calculation of the ionic structure factor to systems without cubic symmetry and to systems with a basis is completely straightforward. (Special points have been found[9] for systems of hexagonal symmetry, and they can be generated for systems of any symmetry.) The occurrence of one-phonon maxima is equally general. The ability to calculate the $\Lambda_{\alpha\beta}(\underset{\sim}{X}_i)$ by a procedure which avoids a difficult three-dimensional numerical integration should prove valuable in a variety of contexts, including, for example, the self-consistent harmonic theory of phonons[19] and the computation of static lattice Green's functions.[42]

Much of the theory of x-ray scattering from simple metals presented in Section II can be extended to liquid metals. Egelstaff, March and McGill[44] have derived a formula for the x-ray cross section in liquid metals that is identical to Eq. (2.6), except that they do not make the adiabatic approximation in the terms involving the correlation of conduction electrons with the ions. Making that approximation, and introducing the pseudopotential $v(\underset{\sim}{k})$, we conclude that Eq. (2.12) is as valid for liquid metals as it is for crystals.

Finally, our calculation has neglected possible anharmonic effects. Those anharmonic terms which are retained in the self-consistent phonon theory[19] are in a sense taken into account here. The formalism we have presented is not altered by using the self-consistent theory, but the frequencies are changed from their harmonic values. In the case of sodium, this change is small.[25] Other anharmonic effects are not taken into account. For example, the interference between one- and two-phonon scattering can cause a noticeable change[7,45] in $S_{ion}(k)$. As shown by Glyde,[7] however, it amounts to only a small shift in the one-phonon scattering for Na at high temperatures. Since both the anharmonic frequency shifts and the inverse phonon lifetimes become quite

small at low temperatures,[25] the size of this contribution should decrease correspondingly. Interference effects, as well as other effects due to anharmonicity, may of course be of somewhat greater importance in the case of lithium.

APPENDIX

We briefly review the special point method,[8,9] which was designed for the integration of quantities varying slowly over the first Brillouin zone (BZ). Here, by a slight modification, we use it to evaluate the integral of oscillating functions (see Eq. (3.7)).

The general integral to be evaluated is:

$$\frac{1}{N}\sum_{\underset{\sim}{q}}^{BZ} f(\underset{\sim}{q}) = \frac{\Omega_c}{(2\pi)^3}\int_{BZ} d^3q\, f(\underset{\sim}{q}), \tag{A.1}$$

where $f(\underset{\sim}{q})$ is assumed to be invariant under the operations of the crystal point group, and Ω_c is the primitive cell volume. (If $f(\underset{\sim}{q})$ is not symmetric, it can, of course, be easily symmetrized.) One expands $f(\underset{\sim}{q})$ in symmetrized plane waves $A_m(\underset{\sim}{q})$:

$$f(\underset{\sim}{q}) = f_o + \sum_{m=1}^{\infty} f_m A_m(\underset{\sim}{q}), \tag{A.2}$$

with

$$A_m(\underset{\sim}{q}) = \sum_{\underset{\sim}{X};m} e^{i\underset{\sim}{q}\cdot\underset{\sim}{X}} \tag{A.3}$$

and

$$f_m = \frac{1}{N_m}\frac{\Omega_c}{(2\pi)^3}\int_{BZ} d^3q\, f(\underset{\sim}{q})\, A_m(\underset{\sim}{q}). \tag{A.4}$$

$\underset{\sim}{X};m$ refers to all lattice vectors $\underset{\sim}{X}$ with the same length X_m that are related by point group operations. N_m is the number of vectors in this m^{th} shell, and the sum in Eq. (A.2) is ordered so that those shells with lowest X_m come first.

A set $\{\underset{\sim}{q}_i\}$ of special points is defined as a set of n points in the BZ with associated weights α_i which satisfy:

$$\sum_{i=1}^{n} \alpha_i A_m(\underset{\sim}{q}_i) = 0 \qquad \text{for } m = 1, \ldots, N, \tag{A.5}$$

$$\sum_{i=1}^{n} \alpha_i = 1. \tag{A.6}$$

Using Eqs. (A.5) and (A.6) in Eq. (A.2):

$$f_o = \sum_{i=1}^{n} \alpha_i \, f(\underset{\sim}{q}_i) - \sum_{i=1}^{n} \alpha_i A_{N+1}(\underset{\sim}{q}_i) \, f_{N+1} + \ldots \tag{A.7}$$

Since f_o is the desired integral, Eq. (A.7) gives an approximation to the integral consisting of an evaluation of $f(\underset{\sim}{q})$ at a (small) set of points. The first neglected term can be shown to be $\pm f_{N+1}$. Not all coefficients f_m for $m > N$ have been neglected, as Eq. (A.5) is always satisfied for an infinite number of shells. The index of the first shell for which Eq. (A.5) is not satisfied is N+1. With increasing number of points n in the set, both the number and the magnitude of the neglected terms become smaller.

At $T = 0°K$, $\mathrm{Tr}\Lambda_{\alpha\beta}(0) \propto \sum_{\underset{\sim}{q}j} 1/\omega(j\underset{\sim}{q})$ is a smooth function, and we may apply the special point method. Although the expansion coefficients f_m decrease slowly with increasing m for large m, they are much smaller than $\mathrm{Tr}\Lambda_{\alpha\beta}(0)$ itself. Thus we expect increasing the number of special points n to have a small effect on $\mathrm{Tr}\Lambda_{\alpha\beta}(0)$. From Table A-I we see the convergence is more rapid for $T = 0°K$ than for $T = 90°K$.

The calculation of $\Lambda_{\alpha\beta}(\underset{\sim}{X}_i)$, $\underset{\sim}{X}_i \neq 0$ is more troublesome, and we illustrate by examining the Trace of this matrix. Symmetrizing the integral of $\Lambda_{\alpha\beta}(\underset{\sim}{X}_i)$:

$$\mathrm{Tr}\Lambda_{\alpha\beta}(\underset{\sim}{X}_i) \propto \sum_{\underset{\sim}{q}j}^{B\mathbb{Z}} \frac{1}{\omega(j\underset{\sim}{q})} \, A_i \, . \tag{A.8}$$

Applying the special point method to this integral means neglecting some of the coefficients $\mathcal{F}_m$ whose form is (we are at $T = 0°K$):

$$\mathcal{F}_m \propto \sum_{\underset{\sim}{q}j}^{B\mathbb{Z}} \frac{1}{\omega(j\underset{\sim}{q})} \, A_i A_m \, . \tag{A.9}$$

Now $A_i A_m$ is itself a sum of symmetrized plane waves:

$$A_i(\underset{\sim}{q})A_m(\underset{\sim}{q}) = \sum_j a_j(i,m)A_j(\underset{\sim}{q}), \tag{A.10}$$

where the first j for which $a_j(i,m)\neq 0$ is that for which $\underset{\sim}{X}_j = |\underset{\sim}{X}_m - \underset{\sim}{X}_i|$. From Eq.s (A.8)-(A.10) it is clear that the $\bar{F}_m$ for large m will be much less than $\mathrm{Tr}\Lambda_{\alpha\beta}(\underset{\sim}{X}_i)$ only if the $\bar{f}_m$ themselves decrease rapidly with increasing m. This, however, is not the case, for just as in Eq.(3.16),

$$\lim_{X_i\to\infty} \sum_{\underset{\sim}{q}}^{BZ} \frac{1}{\omega(j\underset{\sim}{q})} A_i(\underset{\sim}{q}) \sim \frac{1}{X_i^2} \quad . \tag{A.11}$$

The origin of this behavior is the $\frac{1}{q}$ behavior of $\frac{1}{\omega(j\underset{\sim}{q})}$ as $\underset{\sim}{q}\to 0$.[20,43]

To circumvent this difficulty one must find a matrix $M_{\alpha\beta}(\underset{\sim}{q})$ whose behavior at the origin is the same as that of $\sum_j \frac{1}{\omega(j\underset{\sim}{q})} e_\alpha(j\underset{\sim}{q}) e_\beta(j\underset{\sim}{q})$, and which leads to an integral $\int_{BZ} d^3q\, M_{\alpha\beta}(\underset{\sim}{q}) \cos(\underset{\sim}{q}\cdot\underset{\sim}{X})$ which can be evaluated analytically. Then we write:

$$\Lambda_{\alpha\beta}(\underset{\sim}{X}_i) = \frac{\hbar}{MN} \sum_{\underset{\sim}{q}}^{BZ} \left[\left(\sum_j \frac{1}{\omega(j\underset{\sim}{q})} e_\alpha(j\underset{\sim}{q})\, e_\beta(j\underset{\sim}{q})\right) - M_{\alpha\beta}(\underset{\sim}{q})\right] \cos(\underset{\sim}{q}\cdot\underset{\sim}{X}_i)$$

$$+ \frac{\hbar}{MN} \sum_{\underset{\sim}{q}}^{BZ} M_{\alpha\beta}(\underset{\sim}{q}) \cos(\underset{\sim}{q}\cdot\underset{\sim}{X}_i), \tag{A.12}$$

and compute the first integral by the special point method. Since the integrand has no troublesome $\frac{1}{q}$ behavior, its expansion coefficients $\bar{f}_m$ should then decrease rapidly, and the number of special points then needed for an accurate determination of $\Lambda_{\alpha\beta}(\underset{\sim}{X}_i)$ should be (and is in fact) correspondingly small.

To simplify the calculation, we have actually only treated the Trace of $\Lambda_{\alpha\beta}(\underset{\sim}{X}_i)$ in the above fashion, subtracting off a function $M(\underset{\sim}{q})$ whose behavior as $\underset{\sim}{q}\to 0$ is approximately that of $\frac{1}{3}\sum_j \frac{1}{\omega(j\underset{\sim}{q})}$. (As $\underset{\sim}{q}\to 0$, $\sum_j \frac{1}{\omega(j\underset{\sim}{q})} \to \frac{1}{d(\hat{q})q}$, where $d(\hat{q})$ is a function of direction. We have approximated

$d(\hat{q})$ with $\left(\sum_j \int d\Omega_q \frac{1}{c_j(\hat{q})}\right)^{-1}$, where the $c_j(\hat{q})$ are the three speeds of sound.) Tables A-I and A-II show the elements of $\Lambda_{\alpha\beta}(\underset{\sim}{X}_i)$, for $\underset{\sim}{X}_i$ in the first shells (T = 0°K), $Tr\Lambda_{\alpha\beta}(\underset{\sim}{X}_i)$, and $\Lambda_{\alpha\beta}(0)$ for T = 0°K and T = 90°K. Three different (bcc) special point sets were used, with n = 8, 40, and 240. Although one can only expect $Tr\Lambda_{\alpha\beta}(\underset{\sim}{X}_i)$ to converge well, the individual matrix elements also show good convergence.

References

* Work supported by the National Science Foundation (Grant DMR 74-23494), NASA (Contract NGR-33-010-188), and the Materials Science Center (Grant DMR72-03029).

1. R. Colella and B. W. Batterman, Phys. Rev. B 1, 3913(1970).
2. C. B. Walker, Phys. Rev. 103, 547(1956).
3. S. L. Schuster and J. W. Weymouth, Phys. Rev. B 3, 4143(1971).
4. A. A. Maradudin, E. W. Montroll, G. H. Weiss and I. P. Ipatova, in Solid State Physics, ed. by H. Ehrenreich, F. Seitz and D. Turnbull (Academic, New York, 1971), Supplement 3, 2nd ed.
5. G. Albanese and C. Ghezzi, Phys. Rev. B 8, 1315(1973).
6. Y. Kashiwase and J. Harada, J. Phys. Soc. Jap. 35, 1711(1973).
7. H. R. Glyde, Can. J. Phys. 52, 2281(1974).
8. A. Baldereschi, Phys. Rev. B 7, 5212(1973).
9. D. J. Chadi and Marvin L. Cohen, Phys. Rev. B 8, 5747(1973).
10. A. Sjölander, in Phonons and Phonon Interactions, ed. by T. A. Bak (Benjamin, New York, 1964).
11. P. Nozieres and D. Pines, Phys. Rev. 113, 1254(1959).
12. L. Van Hove, Phys. Rev. 95, 249(1954).
13. D. Pines and P. Nozieres, The Theory of Quantum Liquids (Benjamin, New York, 1966), Vol. I.
14. For a discussion of the one-phonon cross section when this is no longer the case, see Ref. 15. This calculation is not restricted to weak pseudopotentials, but agrees with the one-phonon contribution to Eq. (2.6) in the appropriate limit.
15. P. M. Platzman and N. Tzoar, Phys. Rev. B 7, 2450(1973).

16. C.B.Walker, Phys. Rev. 103, 558 (1956).

17. For a liquid metal, the free electron structure factor is a rough approximation to the true one. See Ref.18.

18. J. Chihara, in The Properties of Liquid Metals, ed. by S. Takeuchi, Proceedings of Second International Conference, Tokyo (Taylor and Francis, London, 1973), p.137.

19. P. Choquard, The Anharmonic Crystal (Benjamin, New York, 1971).

20. G.A. Wolfe and B. Goodman, Phys. Rev. 178, 1171 (1969).

21. T.R. Lomer, Proc. Phys. Soc. Lond. 89, 135 (1966).

22. S.V. Semenovskaya and Ya.S. Umanskii, Fiz.Tverd.Tela 6, 2963 (1964) [Sov. Phys. - Solid State 6, 2362 (1965)].

23. J.S. Reid and T. Smith, J. Phys.C 3, 1513 (1970).

24. A.D.B. Woods, B.N. Brockhouse, R.H. March, A.T. Stewart and R. Bowers, Phys. Rev. 128, 1112 (1962).

25. H.R. Glyde and R. Taylor, Phys. Rev. B 5, 1206 (1972).

26. We neglect thermal expansion.

27. By applying the special point method carefully (see the Appendix), it is of course straightforward to calculate the $\Lambda_{\alpha\beta}(\underset{\sim}{X}_i)$ at any temperature.

28. R.W.G. Wyckoff, Crystal Structures (Interscience Publishers, New York, 1963), 2nd ed., Vol.I, p.16.

29. H.G. Smith, G. Dolling, R.M. Nicklow, P.R. Vijayaraghavan and M.K. Wilkinson, in Neutron Inelastic Scattering (International Atomic Energy Agency, Vienna, 1968), Vol.I, p.149.

30. International Tables for X Ray Crystallography (Kynoch Press, Birmingham, England, 1962), Vol.III, p.202.

31. D.J.W. Geldart and S.H. Vosko, Can.J.Phys. 44, 2137 (1966).

32. N.W. Ashcroft, Phys.Lett. 23, 48 (1966); J. Phys. C. 1, 232 (1968).

33. For other examples of this behavior see Ref.s 34-36. The "extra spots" in the x-ray photographs of Ref.34 correspond to this one-phonon structure.

34. M. Born, Rep. Prog. Phys. 9, 294 (1942-43).

35. Y. Kashiwase, J. Phys. Soc. Jap. 34, 1303 (1973).

36. J.E. Eldridge and T.R. Lomer, Proc. Phys. Soc. Lond. 91, 459 (1967).

37. All $\underset{\sim}{k}$ vectors are quoted in units of $2\pi/a$, where a is the lattice constant.

38. R. Comès, in Lecture Notes in Physics: One-Dimensional Conductors, ed. by J. Ehlers, K. Hepp, and H.A. Weidenmüller (Springer-Verlag, Berlin, 1975) Vol.34.

39. Ref.15 stresses precisely this point.

40. N.W. Ashcroft and David C. Langreth, Phys. Rev. 155, 682 (1967).

41. Ref.5 similarly divides the multi-phonon scattering.

42. In this case we do not need $\Lambda_{\alpha\beta}(\underset{\sim}{X}_i)$ but a very similar integral. See Ref.43.

43. H.R. Schober, M. Mostoller, and P.H. Dederichs, Phys. Status Solidi B 64, 173 (1974).

44. P.A. Egelstaff, N.H. March and N.C. McGill, Can. J. Phys. 52, 1651 (1974).

45. W. J. L. Buyers and T. Smith, Phys. Rev. 150, 758(1966);
R. A. Cowley and W. J. L. Buyers, J. Phys. C 2, 2262(1969);
R. A. Cowley, E. C. Svensson, and W. J. L. Buyers, Phys. Rev. Lett. 23, 325(1969).

FIGURE CAPTIONS

Fig. 1 Structure factor $S(\underset{\sim}{k})$ and the one-phonon contribution $S_1(\underset{\sim}{k})$ for Na at T=0°K along [100]. For all the structure factor and cross section plots, the ordinate is in absolute units.

Fig. 2 Structure factor $S(\underset{\sim}{k})$ for Na at T=0°K and T=90°K along [100].

Fig. 3 Structure factor $S(\underset{\sim}{k})$ for Na at T=0°K and T=90°K along [110].

Fig. 4 Structure factor $S(\underset{\sim}{k})$ for Na at T=0°K and T=90°K along [110]. Note the expanded vertical scale.

Fig. 5 Structure factor $S(\underset{\sim}{k})$ for Na at T=0°K and T=90°K along [111].

Fig. 6 Structure factor $S(\underset{\sim}{k})$ for Na at T=0°K and T=90°K along [211].

Fig. 7 Structure factor $S(\underset{\sim}{k})$ for Na at T=0°K and T=90°K along [310].

Fig. 8 Structure factor $S(\underset{\sim}{k})$ for ^{6}Li and ^{7}Li at T=0°K along [100].

Fig. 9 Structure factor $S(\underset{\sim}{k})$ for ^{6}Li and ^{7}Li at T=0°K along [110].

Fig.10 Structure factor $S(\underset{\sim}{k})$ for ^{6}Li and ^{7}Li at T=0°K along [111].

Fig.11 Lines of equal value of the function $1/c|\underset{\sim}{q}(\underset{\sim}{k})|$ in a (001) plane of the lattice reciprocal to the bcc lattice. R is the point $\frac{2\pi}{a}(0,0,0)$, P then point $\frac{2\pi}{a}(\frac{3}{2}, \frac{1}{2}, 0)$, and S is the point $\frac{2\pi}{a}(3, 1, 0)$, where a is the lattice constant. The numbers 1.00,0.50,0.33, and 0.25 indicate the relative value of the function.

Fig.12 Cross sections $W(\underset{\sim}{k})$ and $W_a(\underset{\sim}{k})$ for Na at T=0°K along [100].

Fig.13 Cross sections $W(\underset{\sim}{k})$ and $W_a(\underset{\sim}{k})$ for Na at T=0°K along [110].

Fig.14 Cross sections $W(\underset{\sim}{k})$ and $W_a(\underset{\sim}{k})$ for Na at T=0°K along [111].

Fig.15 Cross sections $W(k)$ and $W_a(k)$ for Na at T=0°K along [100]. Note the expanded vertical and horizontal scales, and the position of $k=2k_f$.

Fig.16 Cross section $W(\underset{\sim}{k})$ for ^{7}Li at T=0°K along [110] for two different values of the core radius, r_c=1.06 and r_c=2.00. Note the expanded horizontal scale.

Fig.17 Cross section $W(\underset{\sim}{k})$ for ^{7}Li at T=0°K along [111] for two different values of the core radius, r_c=1.06 and r_c=2.00. Note the expanded vertical and horizontal scales.

Fig.18 Cross section with <u>all</u> Compton scattering subtracted, $W(\underset{\sim}{k})-S_e(\underset{\sim}{k})$, for ^{7}Li at T=0°K along [111], for two different values of the core radius, r_c=1.06 and r_c=2.00. Note the expanded vertical and horizontal scales.

TABLE I. Structure factor of Sodium at T=0°K along [100]. $S(\underset{\sim}{k})$ vs. Q, where $\underset{\sim}{k} = \frac{2\pi}{a} Q\ (1,0,0)$.

Q	S(k)	Q	S(k)	Q	S(k)	Q	S(k)
0.050	3.34E-04	1.950	4.71E-01	3.600	2.32E-01	5.250	3.39E-01
0.100	6.75E-04	1.970	7.94E-01	3.650	2.58E-01	5.300	3.51E-01
0.150	1.03E-03	1.980	1.20E 00	3.700	2.92E-01	5.350	3.65E-01
0.200	1.41E-03	1.998	1.22E 01	3.750	3.41E-01	5.400	3.81E-01
0.250	1.81E-03	2.002	1.22E 01	3.800	4.14E-01	5.450	3.99E-01
0.300	2.25E-03	2.020	1.24E 00	3.850	5.36E-01	5.500	4.20E-01
0.350	2.72E-03	2.030	8.39E-01	3.900	7.82E-01	5.550	4.44E-01
0.400	3.24E-03	2.050	5.16E-01	3.950	1.52E 00	5.600	4.75E-01
0.450	3.81E-03	2.100	2.75E-01	3.970	2.51E 00	5.650	5.14E-01
0.500	4.42E-03	2.150	1.97E-01	3.980	3.75E 00	5.700	5.66E-01
0.550	5.08E-03	2.200	1.59E-01	3.998	3.71E 01	5.750	6.38E-01
0.600	5.78E-03	2.250	1.37E-01	4.002	3.72E 01	5.800	7.45E-01
0.650	6.52E-03	2.300	1.24E-01	4.020	3.80E 00	5.850	9.23E-01
0.700	7.31E-03	2.350	1.16E-01	4.030	2.56E 00	5.900	1.28E 00
0.750	8.14E-03	2.400	1.11E-01	4.050	1.57E 00	5.950	2.34E 00
0.800	9.03E-03	2.450	1.07E-01	4.100	8.40E-01	5.970	3.76E 00
0.850	9.98E-03	2.500	1.05E-01	4.150	6.00E-01	5.980	5.52E 00
0.900	1.10E-02	2.550	1.04E-01	4.200	4.84E-01	5.998	5.33E 01
0.950	1.22E-02	2.600	1.04E-01	4.250	4.17E-01	6.002	5.33E 01
0.970	1.26E-02	2.650	1.04E-01	4.300	3.74E-01	6.020	5.54E 00
0.980	1.29E-02	2.700	1.04E-01	4.350	3.46E-01	6.030	3.77E 00
0.998	1.34E-02	2.750	1.05E-01	4.400	3.27E-01	6.050	2.36E 00
1.002	1.35E-02	2.800	1.06E-01	4.450	3.13E-01	6.100	1.31E 00
1.020	1.40E-02	2.850	1.08E-01	4.500	3.04E-01	6.150	9.69E-01
1.030	1.43E-02	2.900	1.10E-01	4.550	2.97E-01	6.200	8.01E-01
1.050	1.48E-02	2.950	1.13E-01	4.600	2.93E-01	6.250	7.04E-01
1.100	1.64E-02	2.970	1.14E-01	4.650	2.89E-01	6.300	6.42E-01
1.150	1.82E-02	2.980	1.15E-01	4.700	2.87E-01	6.350	6.00E-01
1.200	2.02E-02	2.998	1.16E-01	4.750	2.86E-01	6.400	5.70E-01
1.250	2.25E-02	3.002	1.16E-01	4.800	2.86E-01	6.450	5.49E-01
1.300	2.50E-02	3.020	1.18E-01	4.850	2.87E-01	6.500	5.34E-01
1.350	2.79E-02	3.030	1.18E-01	4.900	2.89E-01	6.550	5.23E-01
1.400	3.11E-02	3.050	1.20E-01	4.950	2.92E-01	6.600	5.15E-01
1.450	3.48E-02	3.100	1.25E-01	4.970	2.94E-01	6.650	5.09E-01
1.500	3.91E-02	3.150	1.31E-01	4.980	2.95E-01	6.700	5.05E-01
1.550	4.43E-02	3.200	1.37E-01	4.998	2.97E-01	6.750	5.02E-01
1.600	5.07E-02	3.250	1.44E-01	5.002	2.97E-01	6.800	5.00E-01
1.650	5.89E-02	3.300	1.52E-01	5.020	2.99E-01	6.850	5.01E-01
1.700	6.98E-02	3.350	1.61E-01	5.030	3.00E-01	6.900	5.02E-01
1.750	8.53E-02	3.400	1.71E-01	5.050	3.03E-01	6.950	5.05E-01
1.800	1.09E-01	3.450	1.83E-01	5.100	3.10E-01	6.970	5.07E-01
1.850	1.48E-01	3.500	1.96E-01	5.150	3.18E-01	6.980	5.08E-01
1.900	2.28E-01	3.550	2.12E-01	5.200	3.28E-01	6.998	5.10E-01

TABLE II. Structure factor of Sodium at T=0°K along [110]. $S(\underset{\sim}{k})$ vs. Q, where $\underset{\sim}{k} = \frac{2\pi}{a} Q\ (1,1,0)$.

Q	S(k)	Q	S(k)	Q	S(k)	Q	S(k)
0.025	1.92E-04	0.975	2.81E-01	1.800	1.27E-01	2.625	1.74E-01
0.050	3.86E-04	0.985	4.76E-01	1.825	1.45E-01	2.650	1.82E-01
0.075	5.83E-04	0.990	7.21E-01	1.850	1.69E-01	2.675	1.91E-01
0.100	7.84E-04	0.999	7.32E 00	1.875	2.03E-01	2.700	2.03E-01
0.125	9.91E-04	1.001	7.35E 00	1.900	2.54E-01	2.725	2.16E-01
0.150	1.21E-03	1.010	7.49E-01	1.925	3.39E-01	2.750	2.33E-01
0.175	1.43E-03	1.015	5.04E-01	1.950	5.09E-01	2.775	2.54E-01
0.200	1.67E-03	1.025	3.09E-01	1.975	1.02E 00	2.800	2.80E-01
0.225	1.92E-03	1.050	1.63E-01	1.985	1.70E 00	2.825	3.14E-01
0.250	2.18E-03	1.075	1.15E-01	1.990	2.56E 00	2.850	3.59E-01
0.275	2.46E-03	1.100	9.14E-02	1.999	2.56E 01	2.875	4.21E-01
0.300	2.76E-03	1.125	7.76E-02	2.001	2.56E 01	2.900	5.14E-01
0.325	3.09E-03	1.150	6.86E-02	2.010	2.60E 00	2.925	6.69E-01
0.350	3.44E-03	1.175	6.26E-02	2.015	1.75E 00	2.950	9.76E-01
0.375	3.82E-03	1.200	5.83E-02	2.025	1.06E 00	2.975	1.90E 00
0.400	4.23E-03	1.225	5.53E-02	2.050	5.55E-01	2.985	3.12E 00
0.425	4.68E-03	1.250	5.31E-02	2.075	3.86E-01	2.990	4.65E 00
0.450	5.17E-03	1.275	5.17E-02	2.100	3.03E-01	2.999	4.60E 01
0.475	5.72E-03	1.300	5.08E-02	2.125	2.54E-01	3.001	4.60E 01
0.485	5.95E-03	1.325	5.03E-02	2.150	2.22E-01	3.010	4.69E 00
0.490	6.07E-03	1.350	5.01E-02	2.175	1.99E-01	3.015	3.16E 00
0.499	6.29E-03	1.375	5.04E-02	2.200	1.83E-01	3.025	1.94E 00
0.501	6.34E-03	1.400	5.09E-02	2.225	1.71E-01	3.050	1.02E 00
0.510	6.57E-03	1.425	5.17E-02	2.250	1.63E-01	3.075	7.18E-01
0.515	6.70E-03	1.450	5.28E-02	2.275	1.56E-01	3.100	5.68E-01
0.525	6.98E-03	1.475	5.41E-02	2.300	1.51E-01	3.125	4.79E-01
0.550	7.72E-03	1.485	5.48E-02	2.325	1.48E-01	3.150	4.20E-01
0.575	8.56E-03	1.490	5.51E-02	2.350	1.45E-01	3.175	3.79E-01
0.600	9.50E-03	1.499	5.57E-02	2.375	1.44E-01	3.200	3.50E-01
0.625	1.06E-02	1.501	5.59E-02	2.400	1.44E-01	3.225	3.27E-01
0.650	1.18E-02	1.510	5.65E-02	2.425	1.44E-01	3.250	3.10E-01
0.675	1.33E-02	1.515	5.69E-02	2.450	1.45E-01	3.275	2.98E-01
0.700	1.50E-02	1.525	5.78E-02	2.475	1.47E-01	3.300	2.88E-01
0.725	1.70E-02	1.550	6.01E-02	2.485	1.48E-01	3.325	2.81E-01
0.750	1.95E-02	1.575	6.28E-02	2.490	1.48E-01	3.350	2.76E-01
0.775	2.25E-02	1.600	6.60E-02	2.499	1.49E-01	3.375	2.73E-01
0.800	2.63E-02	1.625	6.98E-02	2.501	1.49E-01	3.400	2.71E-01
0.825	3.13E-02	1.650	7.41E-02	2.510	1.50E-01	3.425	2.70E-01
0.850	3.81E-02	1.675	7.93E-02	2.515	1.51E-01	3.450	2.71E-01
0.875	4.76E-02	1.700	8.54E-02	2.525	1.52E-01	3.475	2.73E-01
0.900	6.19E-02	1.725	9.27E-02	2.550	1.56E-01	3.485	2.74E-01
0.925	8.61E-02	1.750	1.02E-01	2.575	1.61E-01	3.490	2.74E-01
0.950	1.35E-01	1.775	1.13E-01	2.600	1.67E-01	3.499	2.75E-01

TABLE III. Structure factor of Sodium at T=0°K along [111]. $S(\underset{\sim}{k})$ vs. Q, where $\underset{\sim}{k} = \frac{2\pi}{a} Q(1,1,1)$.

Q	S(k)	Q	S(k)	Q	S(k)	Q	S(k)
0.050	4.51E-04	1.950	5.63E-01	3.600	4.31E-01	5.250	8.93E-01
0.100	9.31E-04	1.970	9.24E-01	3.650	4.36E-01	5.300	9.63E-01
0.150	1.47E-03	1.980	1.38E 00	3.700	4.52E-01	5.350	9.62E-01
0.200	2.11E-03	1.998	1.36E 01	3.750	4.81E-01	5.400	9.03E-01
0.250	2.90E-03	2.002	1.36E 01	3.800	5.32E-01	5.450	8.40E-01
0.300	3.88E-03	2.020	1.42E 00	3.850	6.24E-01	5.500	7.94E-01
0.350	5.14E-03	2.030	9.68E-01	3.900	8.03E-01	5.550	7.65E-01
0.400	6.80E-03	2.050	6.09E-01	3.950	1.30E 00	5.600	7.52E-01
0.450	9.11E-03	2.100	3.45E-01	3.970	1.95E 00	5.650	7.54E-01
0.500	1.24E-02	2.150	2.62E-01	3.980	2.75E 00	5.700	7.66E-01
0.550	1.75E-02	2.200	2.26E-01	3.998	2.44E 01	5.750	7.88E-01
0.600	2.50E-02	2.250	2.10E-01	4.002	2.44E 01	5.800	8.28E-01
0.650	3.47E-02	2.300	2.05E-01	4.020	2.76E 00	5.850	8.96E-01
0.700	4.09E-02	2.350	2.09E-01	4.030	1.96E 00	5.900	1.02E 00
0.750	4.02E-02	2.400	2.20E-01	4.050	1.32E 00	5.950	1.33E 00
0.800	3.73E-02	2.450	2.39E-01	4.100	8.41E-01	5.970	1.71E 00
0.850	3.56E-02	2.500	2.71E-01	4.150	6.79E-01	5.980	2.18E 00
0.900	3.54E-02	2.550	3.19E-01	4.200	6.04E-01	5.998	1.47E 01
0.950	3.67E-02	2.600	3.85E-01	4.250	5.70E-01	6.002	1.47E 01
0.970	3.77E-02	2.650	4.56E-01	4.300	5.58E-01	6.020	2.16E 00
0.980	3.83E-02	2.700	4.76E-01	4.350	5.59E-01	6.030	1.69E 00
0.998	3.96E-02	2.750	4.30E-01	4.400	5.73E-01	6.050	1.32E 00
1.002	3.99E-02	2.800	3.75E-01	4.450	6.01E-01	6.100	1.03E 00
1.020	4.15E-02	2.850	3.36E-01	4.500	6.48E-01	6.150	9.20E-01
1.030	4.25E-02	2.900	3.15E-01	4.550	7.15E-01	6.200	8.66E-01
1.050	4.47E-02	2.950	3.07E-01	4.600	8.01E-01	6.250	8.41E-01
1.100	5.24E-02	2.970	3.07E-01	4.650	8.83E-01	6.300	8.32E-01
1.150	6.41E-02	2.980	3.08E-01	4.700	8.97E-01	6.350	8.32E-01
1.200	8.21E-02	2.998	3.11E-01	4.750	8.32E-01	6.400	8.41E-01
1.250	1.08E-01	3.002	3.11E-01	4.800	7.55E-01	6.450	8.61E-01
1.300	1.35E-01	3.020	3.15E-01	4.850	6.99E-01	6.500	8.93E-01
1.350	1.42E-01	3.030	3.18E-01	4.900	6.66E-01	6.550	9.35E-01
1.400	1.30E-01	3.050	3.25E-01	4.950	6.54E-01	6.600	9.82E-01
1.450	1.16E-01	3.100	3.51E-01	4.970	6.53E-01	6.650	1.02E 00
1.500	1.07E-01	3.150	3.94E-01	4.980	6.53E-01	6.700	1.03E 00
1.550	1.03E-01	3.200	4.60E-01	4.998	6.55E-01	6.750	9.89E-01
1.600	1.04E-01	3.250	5.48E-01	5.002	6.56E-01	6.800	9.45E-01
1.650	1.09E-01	3.300	6.29E-01	5.020	6.59E-01	6.850	9.12E-01
1.700	1.18E-01	3.350	6.33E-01	5.030	6.62E-01	6.900	8.91E-01
1.750	1.33E-01	3.400	5.71E-01	5.050	6.69E-01	6.950	8.83E-01
1.800	1.57E-01	3.450	5.08E-01	5.100	6.96E-01	6.970	8.83E-01
1.850	2.01E-01	3.500	4.65E-01	5.150	7.42E-01	6.980	8.83E-01
1.900	2.91E-01	3.550	4.40E-01	5.200	8.10E-01	6.998	8.84E-01

TABLE IV. Structure factor of Lithium-7 at T=0°K along [111]. $S(\underset{\sim}{k})$ vs. Q, where $\underset{\sim}{k} = \frac{2\pi}{a} Q(1,1,1)$.

Q	S(k)	Q	S(k)	Q	S(k)	Q	S(k)
0.050	1.02E-03	1.950	1.02E 00	3.600	6.78E-01	5.250	1.01E 00
0.100	2.07E-03	1.970	1.63E 00	3.650	6.86E-01	5.300	1.04E 00
0.150	3.20E-03	1.980	2.39E 00	3.700	7.06E-01	5.350	1.04E 00
0.200	4.46E-03	1.998	2.28E 01	3.750	7.39E-01	5.400	1.01E 00
0.250	5.91E-03	2.002	2.28E 01	3.800	7.93E-01	5.450	9.86E-01
0.300	7.68E-03	2.020	2.43E 00	3.850	8.83E-01	5.500	9.64E-01
0.350	9.94E-03	2.030	1.68E 00	3.900	1.04E 00	5.550	9.50E-01
0.400	1.30E-02	2.050	1.08E 00	3.950	1.40E 00	5.600	9.44E-01
0.450	1.73E-02	2.100	6.33E-01	3.970	1.83E 00	5.650	9.45E-01
0.500	2.38E-02	2.150	4.84E-01	3.980	2.36E 00	5.700	9.50E-01
0.550	3.43E-02	2.200	4.14E-01	3.998	1.65E 01	5.750	9.59E-01
0.600	5.18E-02	2.250	3.82E-01	4.002	1.64E 01	5.800	9.73E-01
0.650	7.70E-02	2.300	3.70E-01	4.020	2.33E 00	5.850	9.95E-01
0.700	9.17E-02	2.350	3.72E-01	4.030	1.80E 00	5.900	1.03E 00
0.750	8.44E-02	2.400	3.86E-01	4.050	1.38E 00	5.950	1.08E 00
0.800	7.47E-02	2.450	4.16E-01	4.100	1.05E 00	5.970	1.13E 00
0.850	6.96E-02	2.500	4.66E-01	4.150	9.19E-01	5.980	1.20E 00
0.900	6.85E-02	2.550	5.44E-01	4.200	8.53E-01	5.998	2.91E 00
0.950	7.09E-02	2.600	6.56E-01	4.250	8.23E-01	6.002	2.89E 00
0.970	7.28E-02	2.650	7.84E-01	4.300	8.12E-01	6.020	1.19E 00
0.980	7.39E-02	2.700	8.14E-01	4.350	8.13E-01	6.030	1.12E 00
0.998	7.63E-02	2.750	7.18E-01	4.400	8.23E-01	6.050	1.07E 00
1.002	7.69E-02	2.800	6.24E-01	4.450	8.46E-01	6.100	1.02E 00
1.020	7.99E-02	2.850	5.64E-01	4.500	8.85E-01	6.150	9.97E-01
1.030	8.18E-02	2.900	5.32E-01	4.550	9.36E-01	6.200	9.84E-01
1.050	8.61E-02	2.950	5.23E-01	4.600	9.95E-01	6.250	9.77E-01
1.100	1.01E-01	2.970	5.24E-01	4.650	1.05E 00	6.300	9.75E-01
1.150	1.24E-01	2.980	5.26E-01	4.700	1.05E 00	6.350	9.76E-01
1.200	1.61E-01	2.998	5.29E-01	4.750	1.00E 00	6.400	9.78E-01
1.250	2.19E-01	3.002	5.30E-01	4.800	9.52E-01	6.450	9.84E-01
1.300	2.87E-01	3.020	5.35E-01	4.850	9.16E-01	6.500	9.91E-01
1.350	2.98E-01	3.030	5.39E-01	4.900	8.96E-01	6.550	1.00E 00
1.400	2.55E-01	3.050	5.48E-01	4.950	8.89E-01	6.600	1.01E 00
1.450	2.18E-01	3.100	5.82E-01	4.970	8.89E-01	6.650	1.01E 00
1.500	1.98E-01	3.150	6.38E-01	4.980	8.89E-01	6.700	1.01E 00
1.550	1.90E-01	3.200	7.24E-01	4.998	8.91E-01	6.750	1.01E 00
1.600	1.91E-01	3.250	8.41E-01	5.002	8.91E-01	6.800	9.99E-01
1.650	2.02E-01	3.300	9.55E-01	5.020	8.93E-01	6.850	9.94E-01
1.700	2.22E-01	3.350	9.52E-01	5.030	8.95E-01	6.900	9.90E-01
1.750	2.52E-01	3.400	8.58E-01	5.050	8.99E-01	6.950	9.89E-01
1.800	3.02E-01	3.450	7.75E-01	5.100	9.15E-01	6.970	9.89E-01
1.850	3.87E-01	3.500	7.19E-01	5.150	9.40E-01	6.980	9.89E-01
1.900	5.53E-01	3.550	6.88E-01	5.200	9.73E-01	6.998	9.89E-01

TABLE A-I. $M^{o} = \frac{1}{2}(2k_f)^2 \Lambda^{o}$ (in units of 10^{-2}).

$M(\underset{\sim}{R}) = \frac{1}{2}(2k_f)^2 \cdot \mathrm{Tr}\, \Lambda_{\alpha\beta}(\underset{\sim}{R})$ (in units of 10^{-2}).

N is the number of special points.

(Na, T=0°K).

N =	8	40	240
$M^{o}(T=0^{o}K)$	3.4367	3.4762	3.4832
$M^{o}(T=90^{o}K)$	7.9897	8.5890	8.8258
$M(\underset{\sim}{R}=(1,1,1))$	1.126	1.134	1.133
$M(\underset{\sim}{R}=(2,0,0))$	0.538	0.541	0.540
$M(\underset{\sim}{R}=(2,2,0))$	0.283	0.261	0.259
$M(\underset{\sim}{R}=(3,1,1))$	0.240	0.223	0.221
$M(\underset{\sim}{R}=(2,2,2))$	0.473	0.479	0.477
$M(\underset{\sim}{R}=(4,0,0))$	0.174	0.167	0.164
$M(\underset{\sim}{R}=(3,3,1))$	0.169	0.152	0.148
$M(\underset{\sim}{R}=(4,2,0))$	0.140	0.099	0.095
$M(\underset{\sim}{R}=(4,2,2))$	0.116	0.137	0.113

TABLE A-II. $M_{\alpha\beta}(\underset{\sim}{R}) = \frac{1}{2}(2k_f)^2 \Lambda_{\alpha\beta}(\underset{\sim}{R})$ (in units of 10^{-3}).

N is the number of special points.

(Na, T=0 °K).

	N	M_{xx}	M_{xy}	M_{yy}	M_{xz}	M_{yz}	M_{zz}
$\underset{\sim}{R}$=(1,1,1)	8	3.754	2.610	3.754	2.610	2.610	3.754
	40	3.780	2.664	3.780	2.664	2.664	3.780
	240	3.778	2.666	3.778	2.666	2.666	3.778
$\underset{\sim}{R}$=(2,0,0)	8	0.822	0	2.278	0	0	2.278
	40	0.716	0	2.345	0	0	2.345
	240	0.708	0	2.345	0	0	2.345
$\underset{\sim}{R}$=(2,2,0)	8	1.278	0.698	1.278	0	0	0.270
	40	1.215	0.740	1.215	0	0	0.184
	240	1.207	0.744	1.207	0	0	0.181
$\underset{\sim}{R}$=(3,1,1)	8	0.715	0.225	0.842	0.225	0.316	0.842
	40	0.557	0.230	0.836	0.230	0.444	0.836
	240	0.541	0.233	0.832	0.233	0.448	0.832
$\underset{\sim}{R}$=(2,2,2)	8	1.578	1.039	1.578	1.039	1.039	1.578
	40	1.598	1.133	1.598	1.133	1.133	1.598
	240	1.589	1.139	1.589	1.139	1.139	1.589
$\underset{\sim}{R}$=(4,0,0)	8	0.581	0	0.581	0	0	0.581
	40	0.212	0	0.727	0	0	0.727
	240	0.186	0	0.730	0	0	0.730
$\underset{\sim}{R}$=(3,3,1)	8	0.680	0.528	0.680	0.073	0.073	0.331
	40	0.668	0.458	0.668	0.120	0.120	0.188
	240	0.653	0.464	0.653	0.125	0.125	0.179
$\underset{\sim}{R}$=(4,2,0)	8	0.465	0.275	0.465	0	0	0.465
	40	0.356	0.167	0.400	0	0	0.234
	240	0.331	0.171	0.391	0	0	0.227
$\underset{\sim}{R}$=(4,2,2)	8	0.388	0.304	0.388	0.304	0	0.388
	40	0.386	0.208	0.491	0.208	0.303	0.491
	240	0.363	0.214	0.482	0.214	0.314	0.482

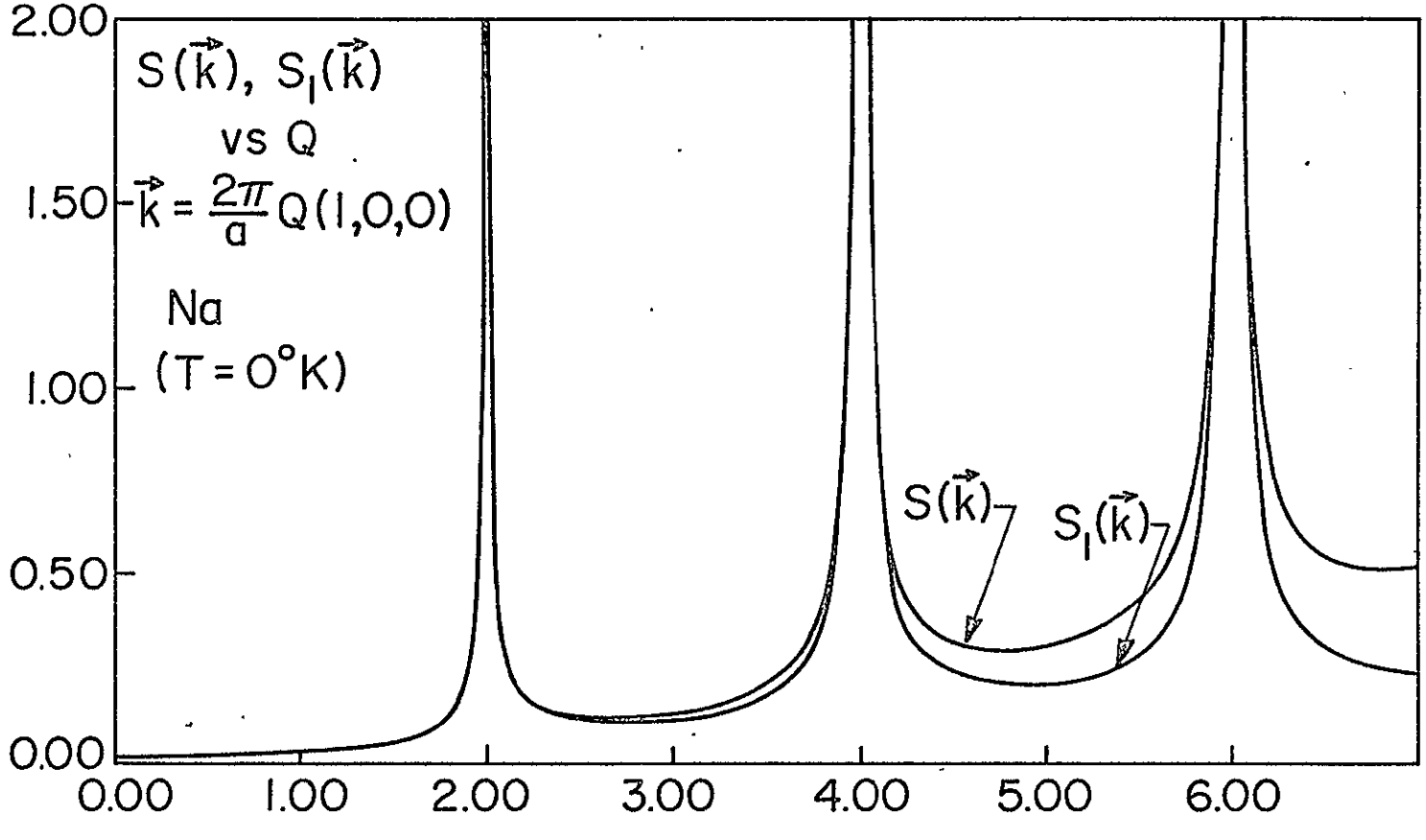
2.00
1.50
1.00
0.50
0.00
S(k), S1(k)
vs Q
k = 2π/a Q(1,0,0)
Na
(T = 0°K)
S(k)
S1(k)
0.00
1.00
2.00
3.00
4.00
5.00
6.00

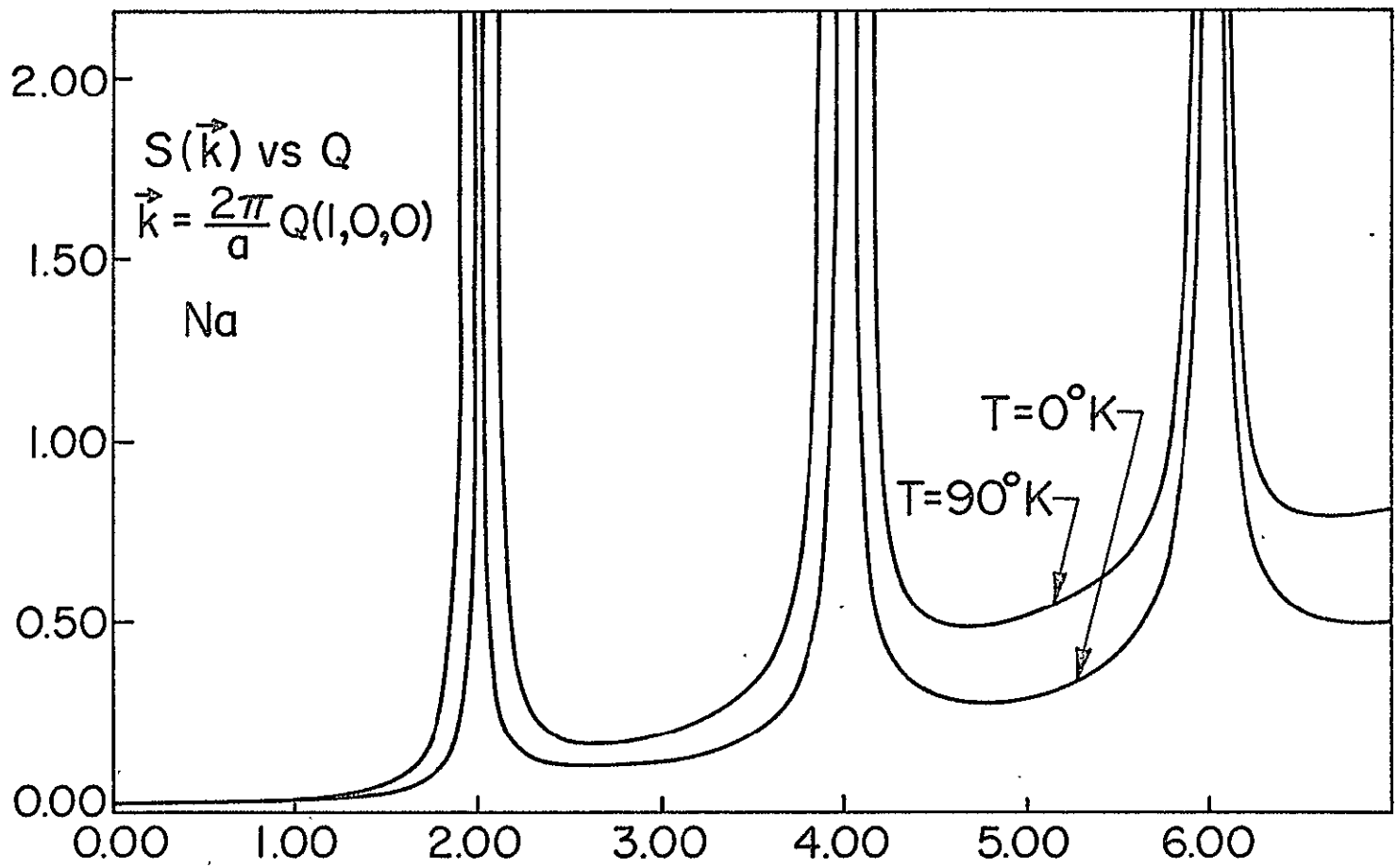
2.00
1.50
1.00
0.50
0.00
S(k) vs Q
k = 2π/a Q(1,0,0)
Na
T=0°K
T=90°K
0.00
1.00
2.00
3.00
4.00
5.00
6.00

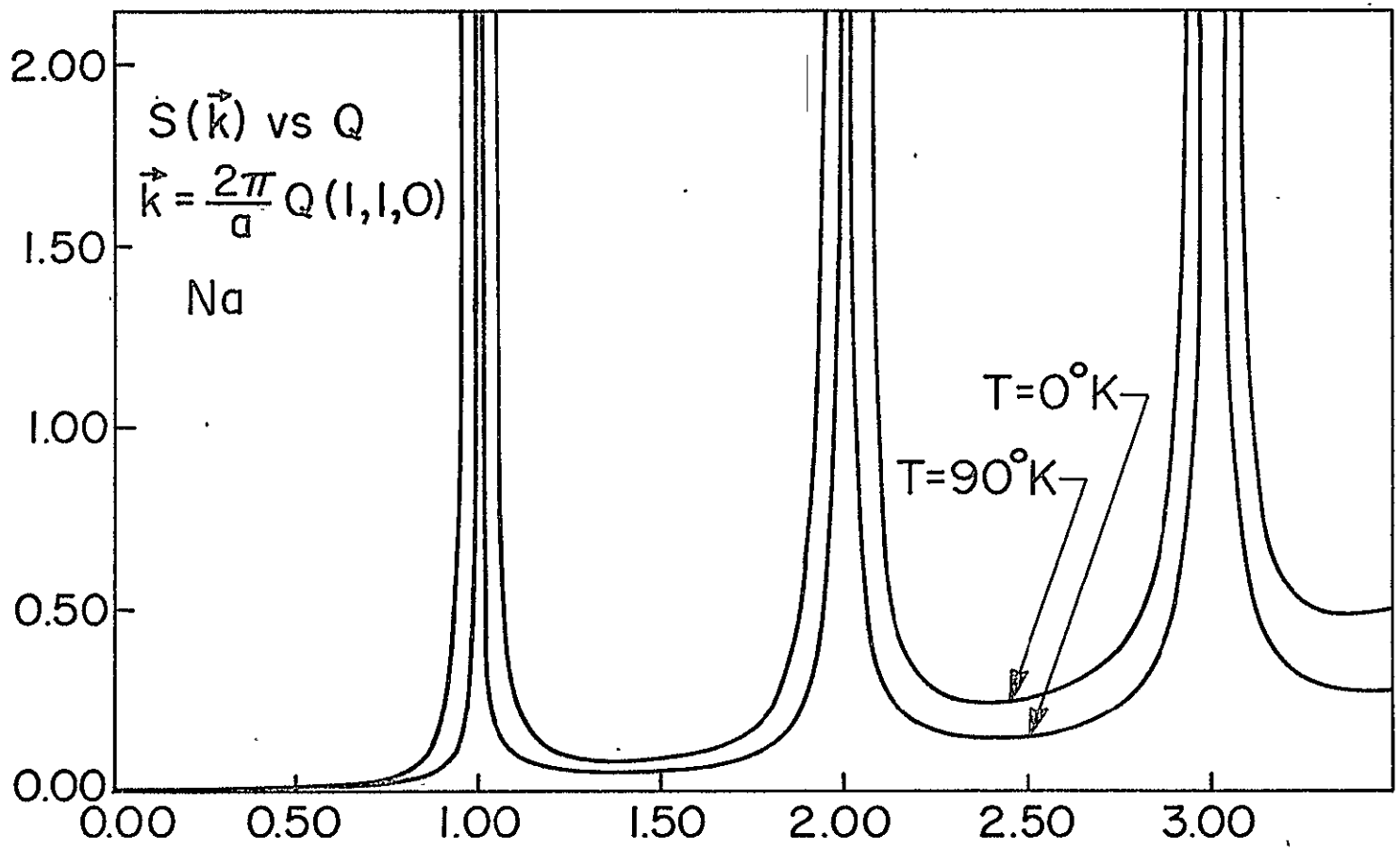
S(k) vs Q
k = 2π/a Q (1,1,0)
Na
T=0°K
T=90°K
2.00
1.50
1.00
0.50
0.00
0.00
0.50
1.00
1.50
2.00
2.50
3.00

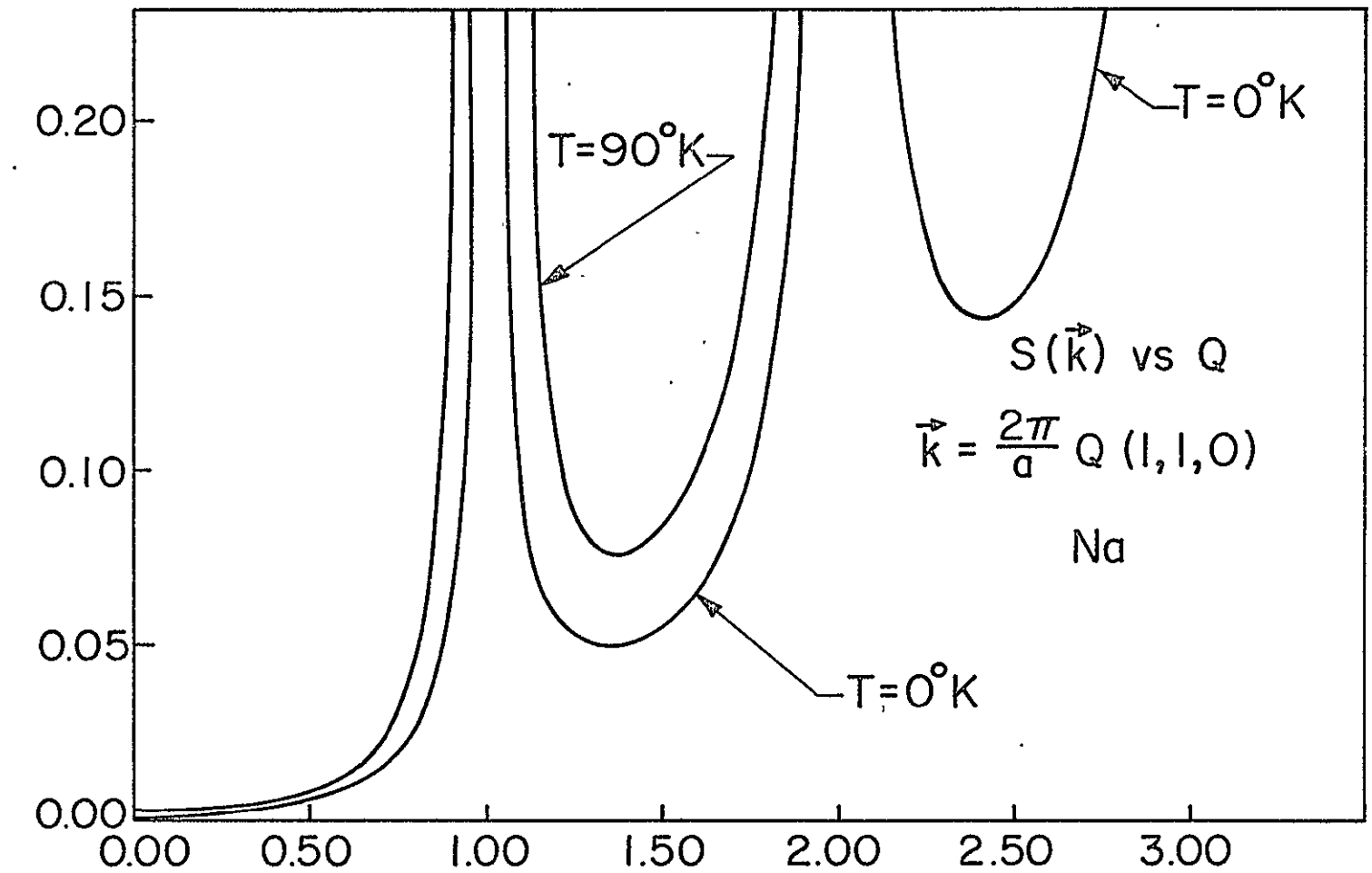
0.20
0.15
0.10
0.05
0.00
0.00
0.50
1.00
1.50
2.00
2.50
3.00
T=90°K
T=0°K
T=0°K
S(k) vs Q
k = 2π/a Q (1,1,0)
Na

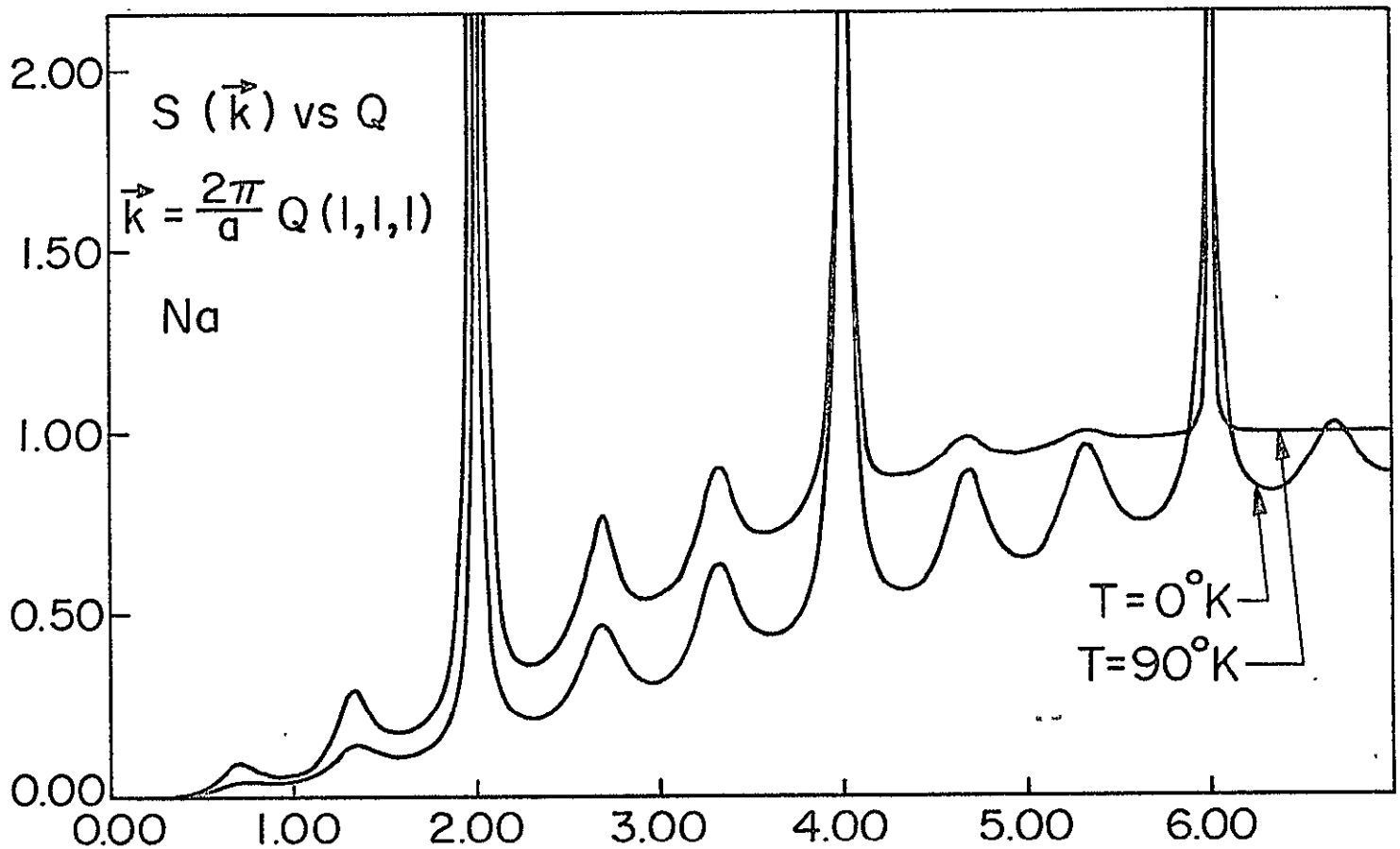
S (k) vs Q
k = 2π/a Q (1,1,1)
Na
T=0°K
T=90°K
2.00
1.50
1.00
0.50
0.00
0.00
1.00
2.00
3.00
4.00
5.00
6.00

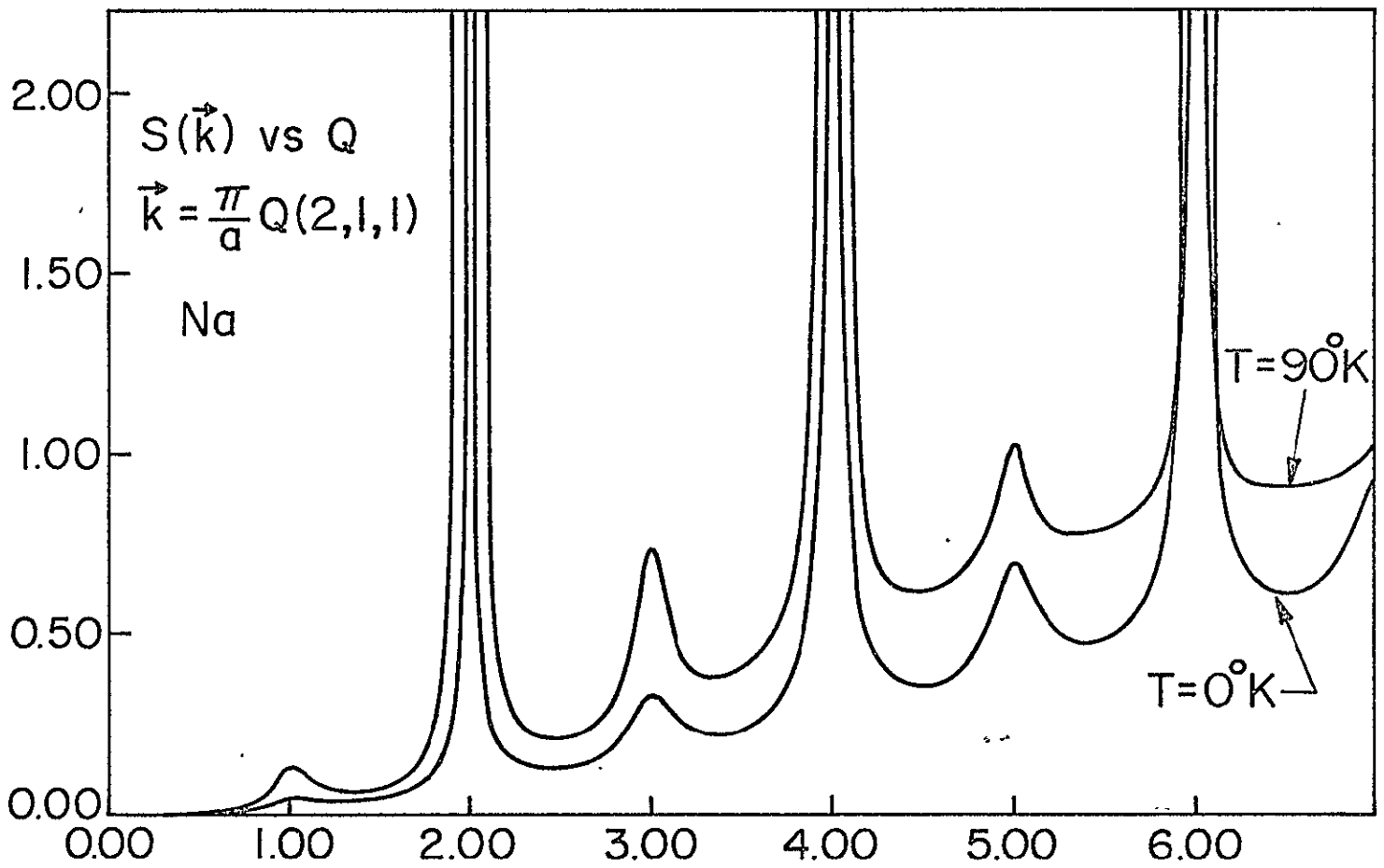
S(k) vs Q
k = π/a Q(2,1,1)
Na
T=90°K
T=0°K
2.00
1.50
1.00
0.50
0.00
0.00
1.00
2.00
3.00
4.00
5.00
6.00

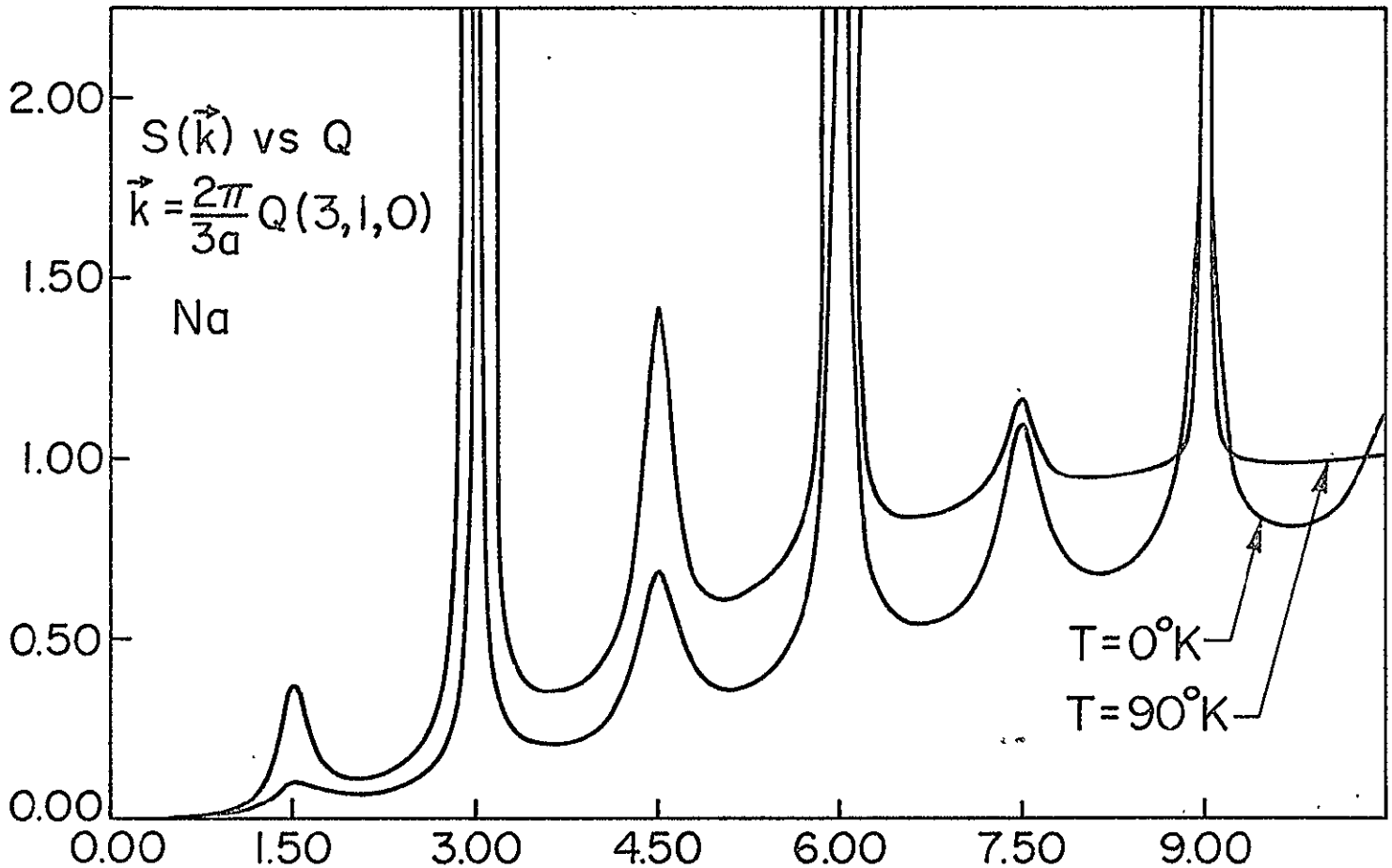
2.00
1.50
1.00
0.50
0.00
S(k) vs Q
k = 2π/3a Q(3,1,0)
Na
T=0°K
T=90°K
0.00
1.50
3.00
4.50
6.00
7.50
9.00

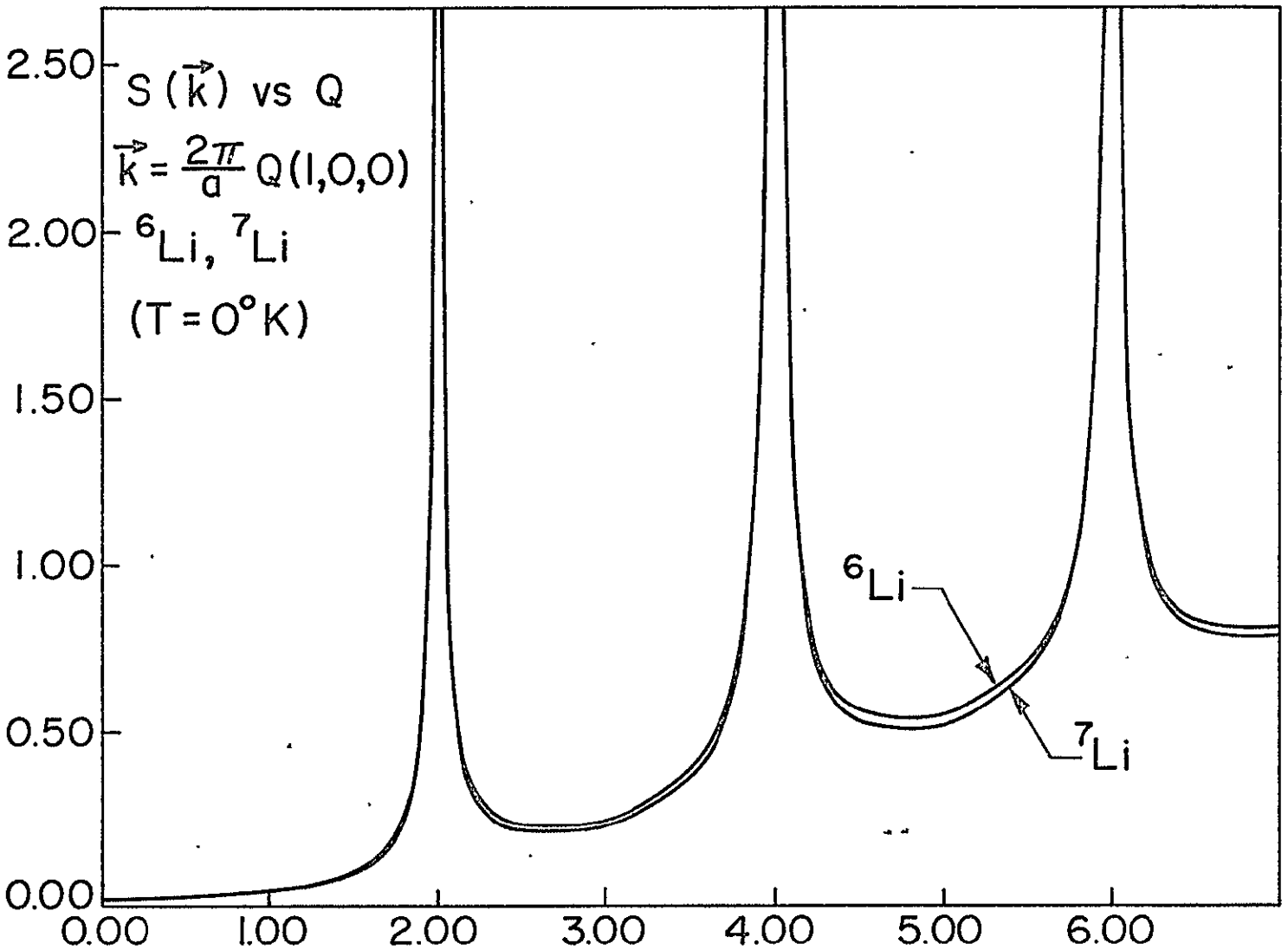
S (k) vs Q
k = 2π/a Q(1,0,0)
6Li, 7Li
(T = 0°K)
2.50
2.00
1.50
1.00
0.50
0.00
0.00
1.00
2.00
3.00
4.00
5.00
6.00
6Li
7Li

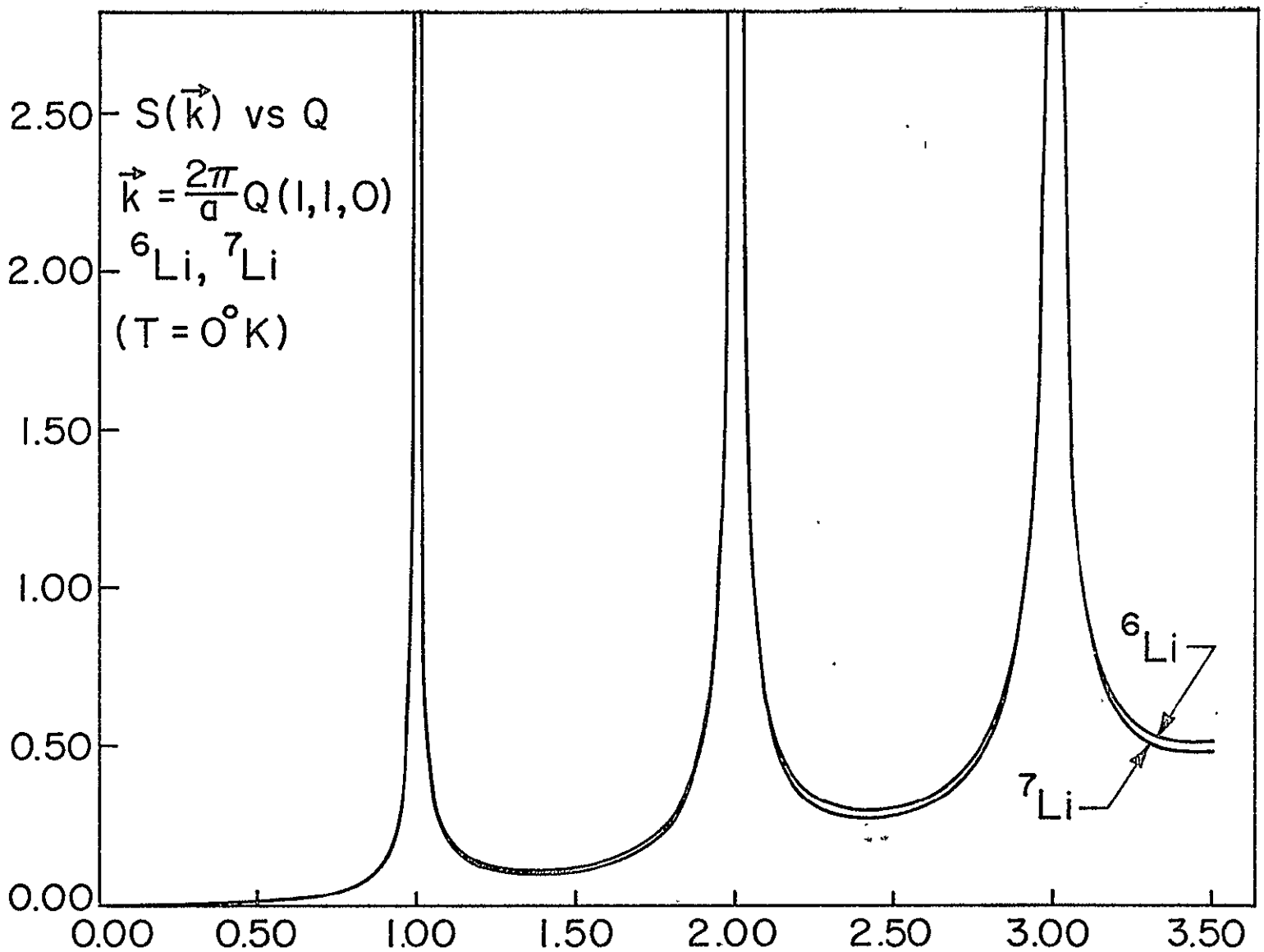
S(k) vs Q
k = 2π/a Q(1,1,0)
6Li, 7Li
(T = 0°K)
2.50
2.00
1.50
1.00
0.50
0.00
0.00
0.50
1.00
1.50
2.00
2.50
3.00
3.50
6Li
7Li

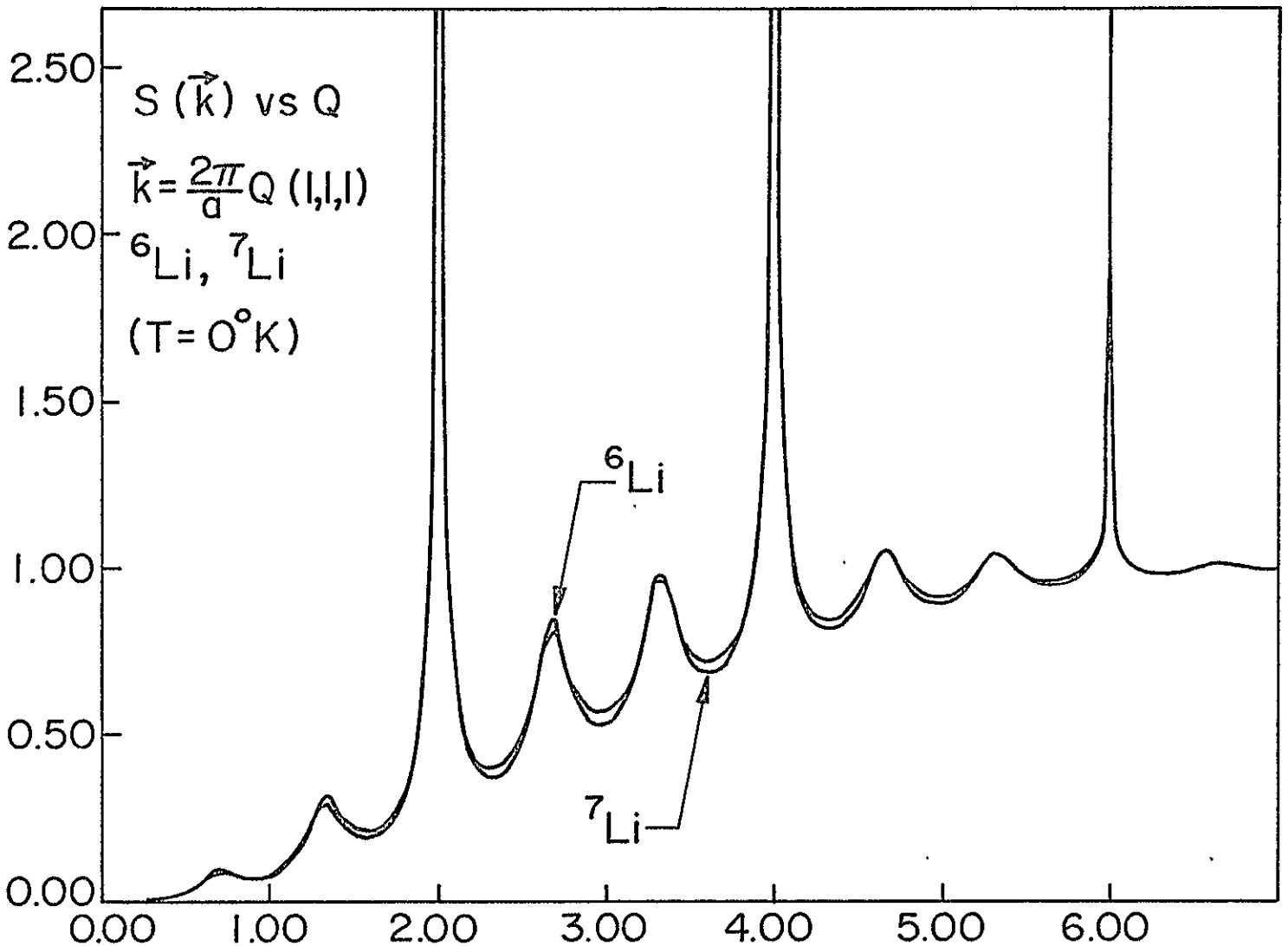
S (k) vs Q
k = 2π/a Q (1,1,1)
6Li, 7Li
(T = 0°K)
6Li
7Li
2.50
2.00
1.50
1.00
0.50
0.00
0.00
1.00
2.00
3.00
4.00
5.00
6.00

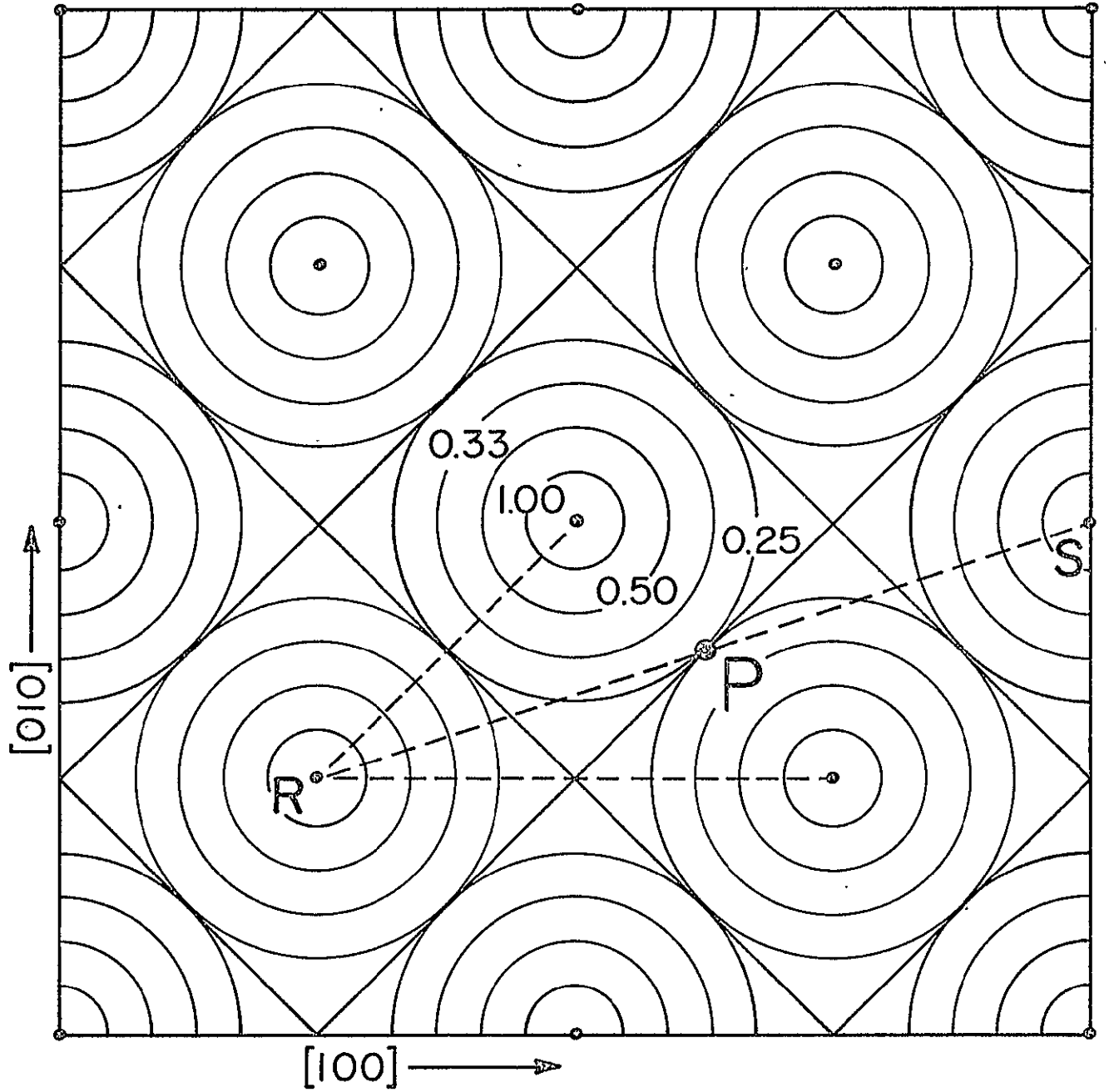
0.33
1.00
0.50
0.25
S
P
R
[010]
[100]

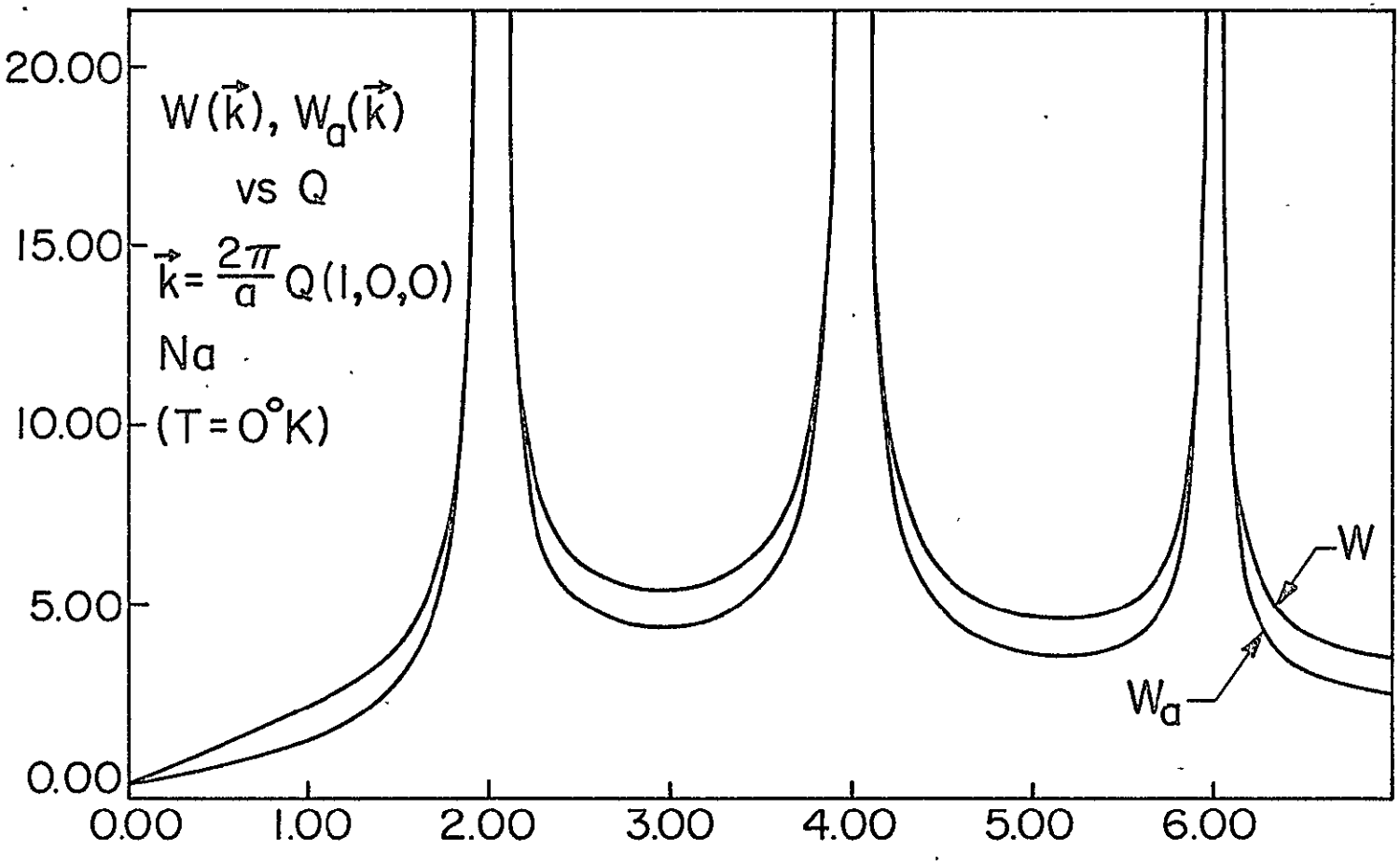
20.00
15.00
10.00
5.00
0.00
$W(\vec{k})$, $W_a(\vec{k})$
vs Q
$\vec{k} = \frac{2\pi}{a} Q(1,0,0)$
Na
(T = 0°K)
W
W_a
0.00
1.00
2.00
3.00
4.00
5.00
6.00

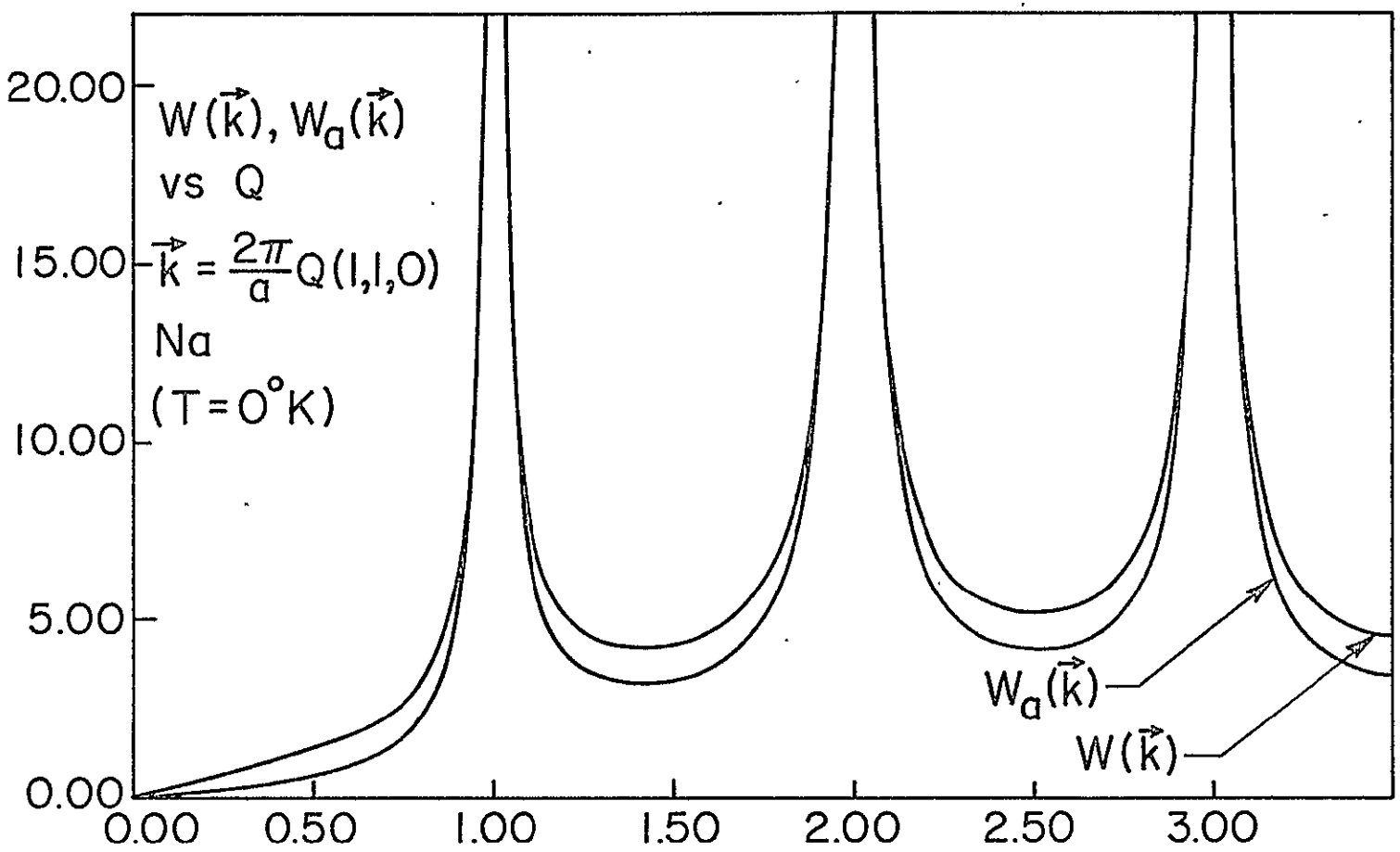
20.00
15.00
10.00
5.00
0.00
W(k), Wa(k)
vs Q
k = 2π/a Q(1,1,0)
Na
(T=0°K)
Wa(k)
W(k)
0.00
0.50
1.00
1.50
2.00
2.50
3.00

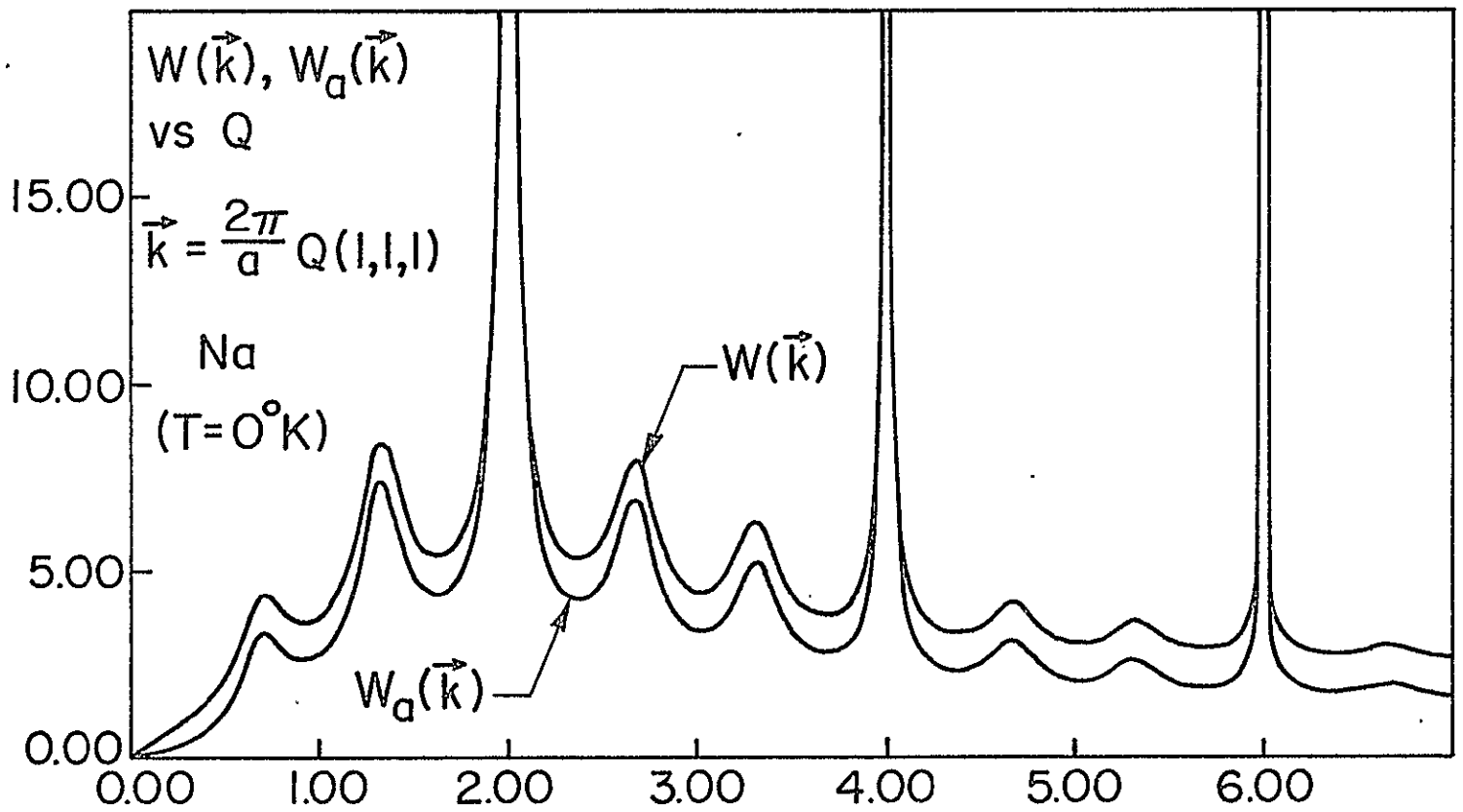
W(k), Wa(k)
vs Q
k = 2π/a Q(1,1,1)
Na
(T=0°K)
W(k)
Wa(k)
15.00
10.00
5.00
0.00
0.00
1.00
2.00
3.00
4.00
5.00
6.00

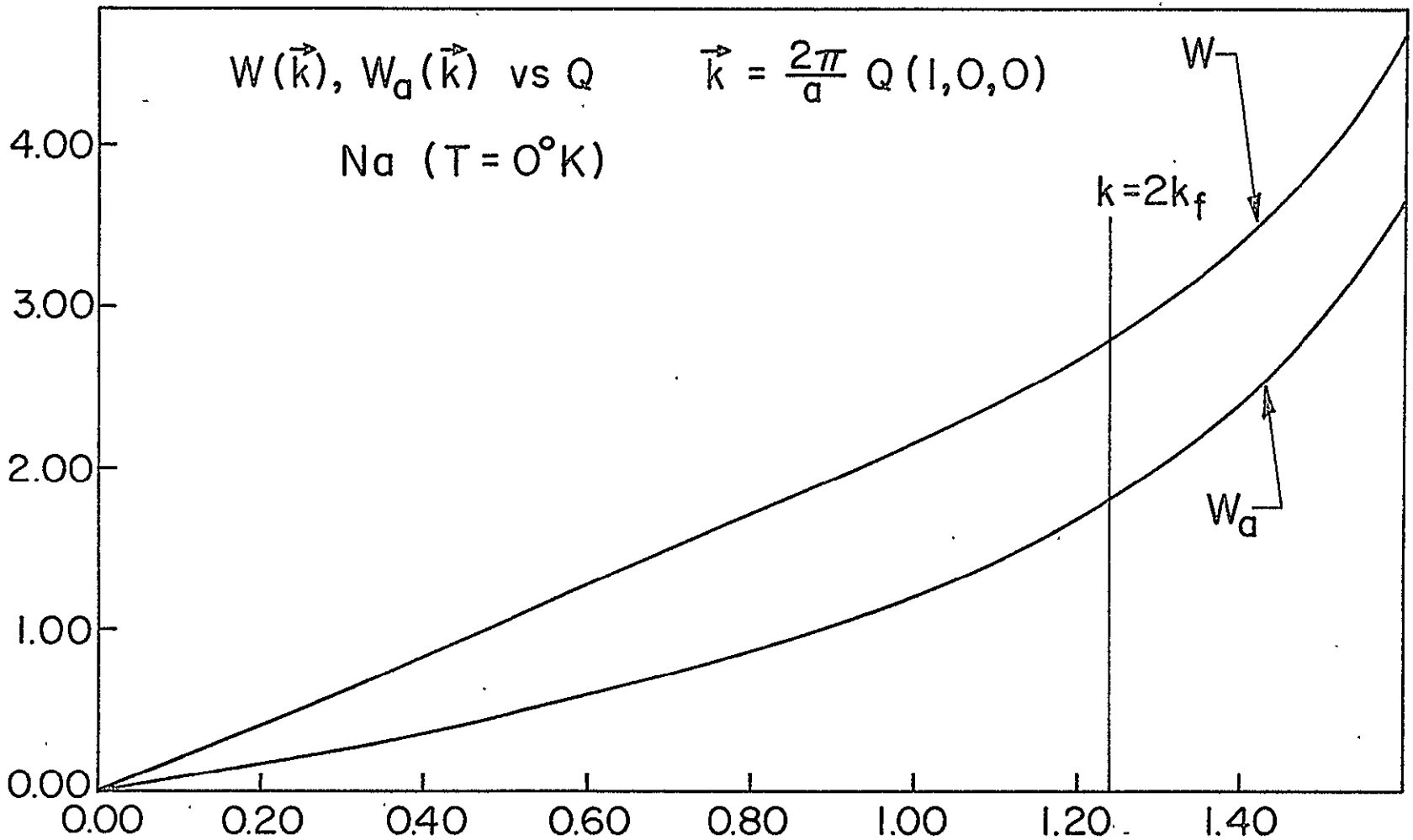
W(k), Wa(k) vs Q
k = 2π/a Q (1,0,0)
Na (T = 0°K)
W
k=2kf
Wa
4.00
3.00
2.00
1.00
0.00
0.00
0.20
0.40
0.60
0.80
1.00
1.20
1.40

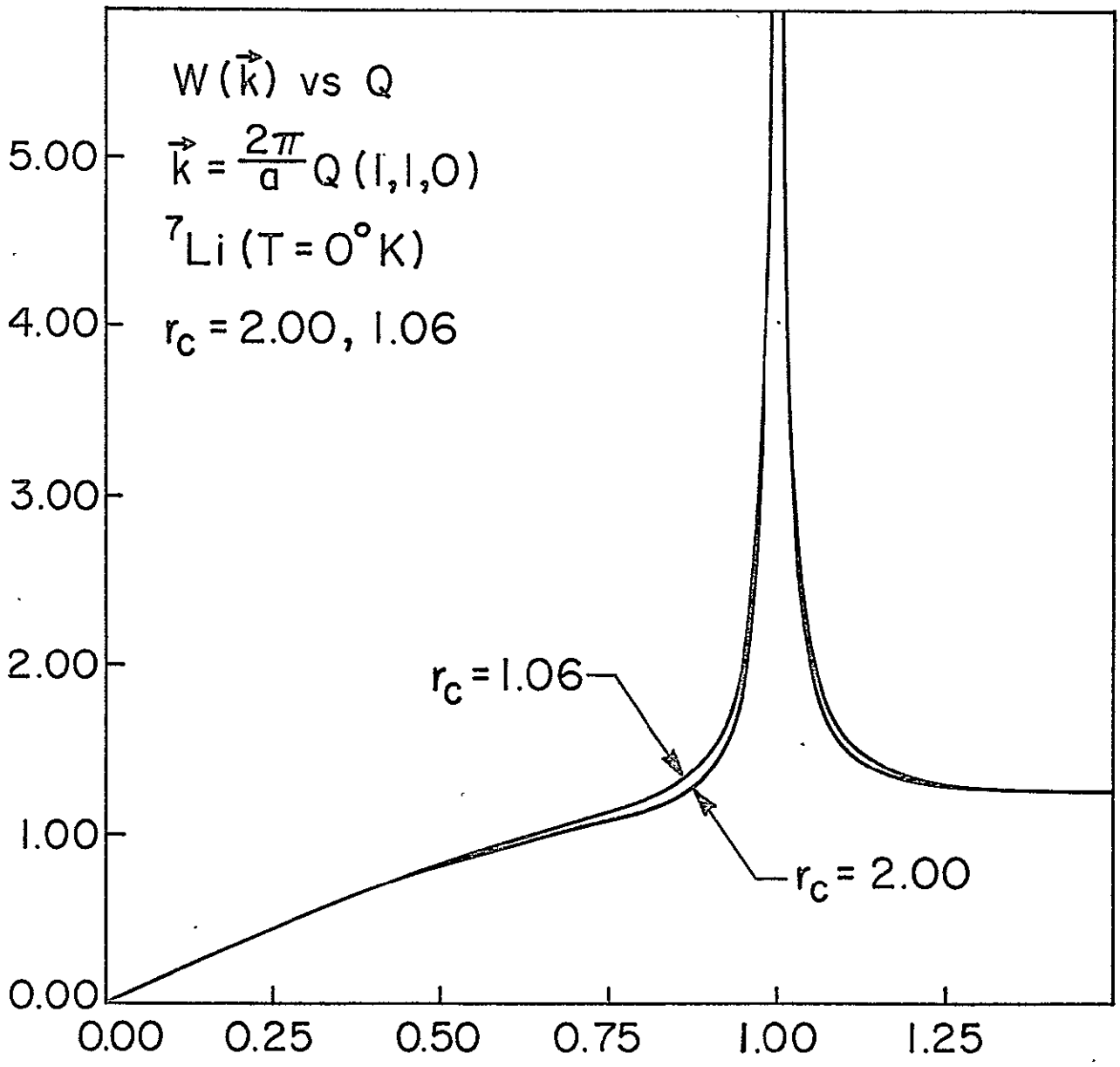
W(k) vs Q
k = 2π/a Q (1,1,0)
7Li (T = 0°K)
rc = 2.00, 1.06
5.00
4.00
3.00
2.00
1.00
0.00
0.00
0.25
0.50
0.75
1.00
1.25
rc = 1.06
rc = 2.00

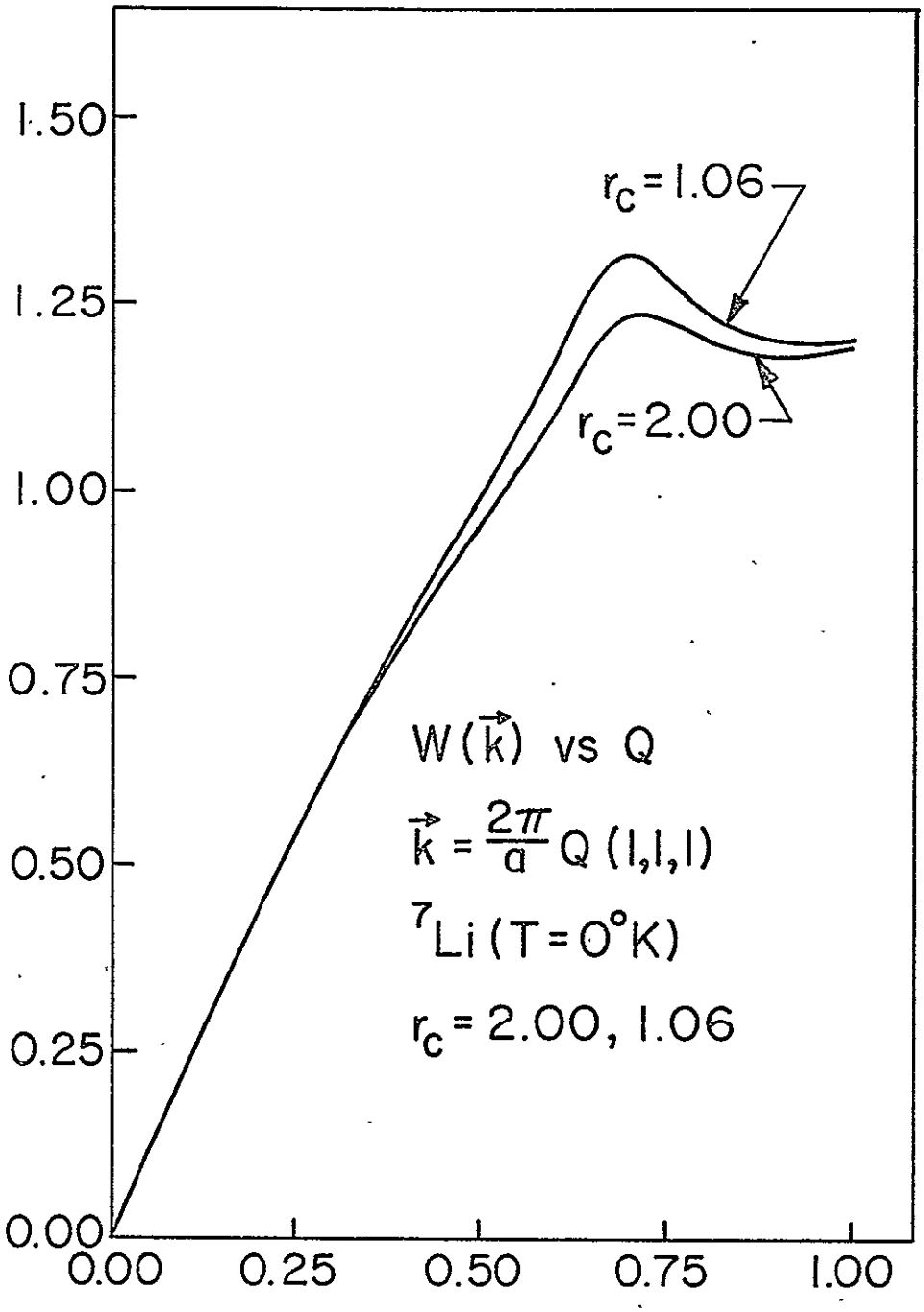
1.50
1.25
1.00
0.75
0.50
0.25
0.00
0.00
0.25
0.50
0.75
1.00
$r_c = 1.06$
$r_c = 2.00$
$W(\vec{k})$ vs Q
$\vec{k} = \frac{2\pi}{a} Q\,(1,1,1)$
$^7Li\,(T = 0^\circ K)$
$r_c = 2.00, 1.06$

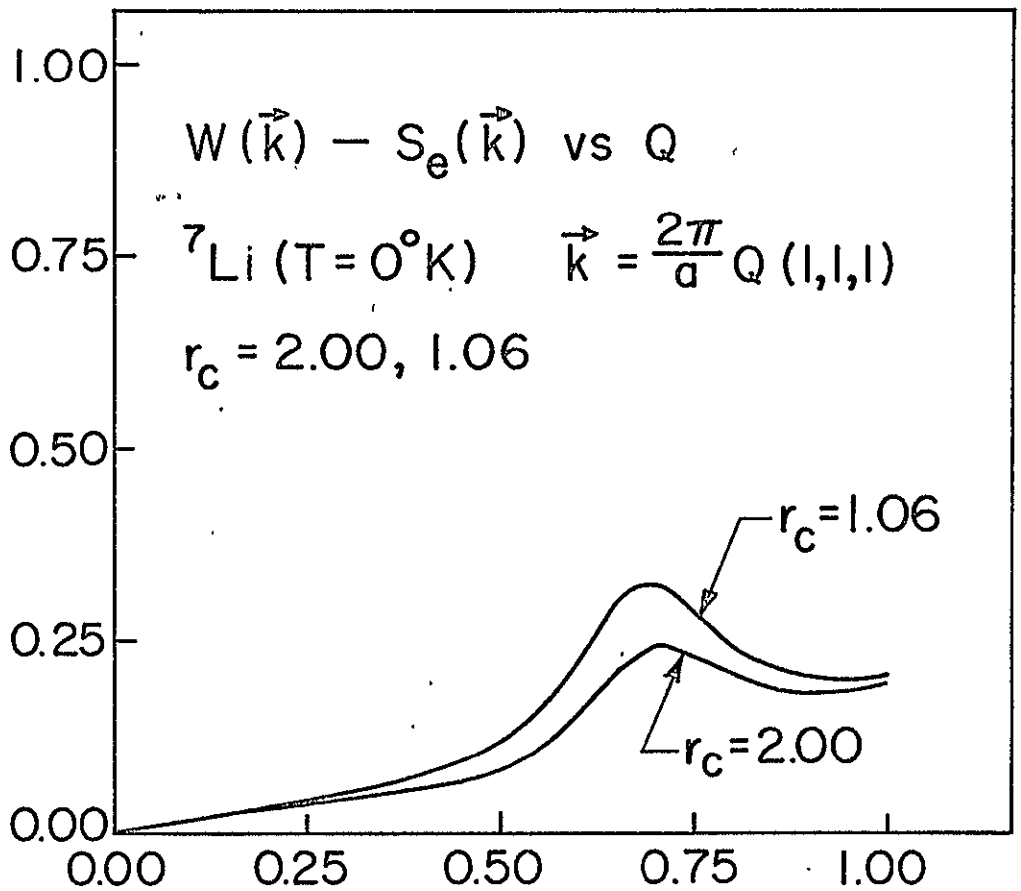
1.00
0.75
0.50
0.25
0.00
0.00
0.25
0.50
0.75
1.00
W(k) − S_e(k) vs Q
⁷Li (T = 0°K)
k = 2π/a Q (1,1,1)
r_c = 2.00, 1.06
r_c = 1.06
r_c = 2.00